ELSEVIER

Journal of Photochemistry and Photobiology A: Chemistry 100 (1996) 15–34

Journal of PHOTOCHEMISTRY AND PHOTOBIOLOGY A:CHEMISTRY

Theoretical studies of intramolecular electron transfer reactions: distance and free energy dependences

Luís G. Arnaut, Sebastião J. Formosinho *,[1]

Chemistry Department, University of Coimbra, 3049 Coimbra Codex, Portugal

Received 7 June 1996; accepted 25 June 1996

Abstract

Electron tunneling through a square potential energy barrier is used to calculate the distance-dependent factors of electron transfer (ET) processes in metal–monolayer–metal junctions, donors and acceptors dispersed in rigid organic glasses, intramolecular ET in rigid donor–bridge–acceptor species in solution and redox centers attached to electrodes through adsorbed monolayers. This tunneling model of distance-dependent non-adiabatic factors is incorporated in the intersecting state model (ISM). The result is a simple semiclassical theory which is used to calculate the rates of non-adiabatic ET reactions. When the electron is originally located in a π^* molecular orbital of the donor and the reaction free energy is no lower than approximately -50 kJ mol^{-1}, no adjustable parameters are necessary to calculate the intramolecular ET rates from a donor, through a rigid bridge, to an acceptor. Such calculated rates are within an order of magnitude of the experimental values. The model can also account for the ET rates of more exothermic reactions provided that the value of an empirical parameter, which is constant for structurally related reactants and solvents of similar polarity, is estimated. The physical meaning of this parameter is related to the dynamics of the reactions. The profiles of the distance and free energy dependences of photoinduced ET rates are closely reproduced. The occurrence of distance-dependent non-adiabatic factors in intermolecular σ^*-d ETs is rationalized.

Keywords: Distance dependence; Free energy dependence; Intramolecular electron transfer; Theoretical studies

1. Introduction

The transfer of an electron from a donor to an acceptor at restricted distances has become a central concern of experimental and theoretical studies on electron transfer (ET) reactions. The relevance of such ET is illustrated by its probable involvement as the first chemical step in photosynthesis, where an electron is transferred from chlorophyll donors to quinone acceptors at restricted distances and orientations [1]. It is also believed that artificial ET systems aiming at the conversion of sunlight into electricity may be designed on the basis of the detailed control of the energetics and kinetics of the donor and acceptor and of the bonding in the molecular bridge which keeps them at controlled geometries [2]. ET in organized systems is also expected to find important applications in the development of molecular electronic devices [3].

The distance between donor and acceptor can be restricted using a great variety of strategies. In 1971, Mann and Kuhn [4] showed that monolayers of fatty acids of different chain lengths between metal electrodes led to an exponential decrease in conductivity vs. thickness. The relatively small tunneling decay coefficient obtained for electrodes of Al and Hg, $\beta_{exp} = 1.49$ Å^{-1}, raised the possibility of performing efficient long-range ET. The initial skepticism towards some of the earlier results, due to the very high sensitivity of the monolayers to imperfections in their structure, was countered by systematic reports giving similar values of β_{exp} for analogous systems [5–8]. Depending on the metal electrodes, the tunneling decay coefficients across monolayers of fatty acids are in the range 1.1–1.6 Å^{-1}. Contemporary work by Miller [9] presented evidence for long-range tunneling of trapped electrons in γ-irradiated organic glasses. A few years later, long-range ET from the biphenyl anion to triphenylethylene in rigid, glassy ethanol was demonstrated [10]. In a subsequent study on the dependence of ET rates on distance and reaction exothermicity, Miller et al. [11] were able to quantify the distance dependence of ET from the biphenyl anion to different acceptors in methyltetrahydrofuran (MTHF) at 77 K, and obtained $\beta_{exp} = 1.20$ Å^{-1}. A recent study by Krongauz [12] using different donors and acceptors in MTHF at 77 K gave a range of β_{exp} values between 0.93

* Corresponding author. Tel.: 351-39-24249; fax: 351-39-27703.

[1] Also at Escola Superior de Ciências e Tecnologia, Universidade Católica Portuguesa, 3500 Viseu, Portugal.

PII S1010-6030(96)04446-2

and 1.36 $Å^{-1}$. However, the most influential experimental study of distance and conformational restrictions in ET was made by Closs et al. [13], who studied intramolecular ET from 4-biphenyl anion covalently linked by rigid bridges of different lengths and conformations to 2-naphthyl. Using their data for the rate constants and edge-to-edge distances of donor and acceptor bonded to equatorial positions in the bridge, we calculate $\beta_{exp} = 1.22$ $Å^{-1}$. Subsequent studies on intramolecular ET by other workers have shown that β_{exp} between covalently linked donors and acceptors may range from 0.8 to 1.4 $Å^{-1}$ [14]. This work inspired electrochemical studies in which an electroactive species was covalently linked to a saturated hydrocarbon containing an anchor group, and this group was adsorbed on the surface of a metal electrode [15]. In these studies, electrochemical unimolecular rate constants were measured and their distance dependence was studied using bridges of different lengths. The measured β_{exp} values were in the range 0.8–1.8 $Å^{-1}$ [16–18]. More recently, Moser et al. [19] showed that the typical tunneling decay coefficient of ET in proteins is $\beta_{exp} = 1.4$ $Å^{-1}$. Given the importance and complexity of biological ET, this subject will be left for a future publication. It is well known that when two redox sites are separated by a conjugated pathway, the values of β_{exp} observed are much lower than 1.2 $Å^{-1}$. In such cases, the energetic proximity between the electron in the highest occupied molecular orbital (HOMO) of the donor and the lowest unoccupied molecular orbital (LUMO) of the bridge and the π symmetry of the orbitals involved favor the electronic coupling between donor and acceptor and lead to mixed valence species with intense intervalence charge transfer absorption bands. These bands are the result of light absorption in which the photon removes an electron from the donor and transfers it across the bridge to the acceptor. The nature of such intramolecular propagation of electrons between a donor and acceptor site across "molecular wires" [20,21] is different from the thermal ET processes across non-conjugated bridges which are the subject of this study, and will not be considered further in this work.

The most striking observation concerning all the experimental studies addressed in this work is that tunneling coefficients of approximately 1.2 $Å^{-1}$ can occur in systems as different as metal–monolayer–metal junctions, donors and acceptors dispersed in rigid organic glasses, intramolecular ET in rigid donor–bridge–acceptor species in solution and redox centers attached to electrodes through adsorbed monolayers. Apparently, the common feature of these systems is that the electron must tunnel from the donor to the acceptor through a region in which its energy is much higher than when it is located on the donor. The nature of the region crossed by the electron varies from small molecules frozen in random positions to long and rigid saturated hydrocarbon chains.

The distance dependence of ET has also been actively investigated theoretically. The first steps in this field were taken by McConnell [22], who discussed the paramagnetic spectra of mononegative ions of α,ω-diphenylalkanes in terms of through-σ-bond electronic interactions. However, it was the work of Hoffmann [23] showing that through-bond coupling over three σ bonds could be very high that motivated further theoretical approaches to this problem. The calculated distance dependence proved to be very sensitive to the method of calculation. The seminal work of McConnell [22] predicted β_{calc} to be larger than 1.8 $Å^{-1}$, while the extended Hückel molecular orbital (MO) of Hoffmann [23] gave $\beta_{calc} = 0.37$ $Å^{-1}$. Some of the reasons behind the discrepancies in the β_{calc} values have been clarified by the ab initio calculations published by Paddon-Row [24], Kim et al. [25], Curtiss et al. [26], Larsson and Braga [27] and Liang and Newton [28]. The coupling mechanism between the HOMO of the donor and the LUMO of the acceptor, taking into detailed account the electronic structure of the bridge, became known as the "superexchange" mechanism, a terminology first introduced by Anderson [29] to name the magnetic interactions between atoms separated from each other by intervening non-magnetic ions. The superexchange mechanism is a through-bond interaction. For each system, it competes with through-space interaction, which is usually interpreted as electron tunneling. The development of the superexchange mechanism was judged to be necessary because modeling the connection between donor and acceptor by a homogeneous medium seemed to yield exceedingly high tunneling barriers and, consequently, overestimates of the tunneling decay coefficient [28]. Although such a development can be regarded as a refinement over the homogeneous treatment of the intervening medium, it ignores the conspicuous incidence of decay coefficients around 1.2 $Å^{-1}$ [30]. The similarity of β_{exp} regardless of the structure of the medium suggests that caution is necessary towards theoretical treatments which are highly dependent on the electronic structure of each bridge, because $\beta_{exp} \approx 1.2$ $Å^{-1}$ is also found in systems in which donor and acceptor are not connected by covalent bonds. A more general approach to the distance dependence of long-range ET is desirable.

Our own interest in this field comes from the application of the intersecting state model (ISM) to chemical reactivity and, more specifically, to ET reactions. In recent applications of this model to ET, we were able to calculate self-exchange rates of metal complexes transferring π-d electrons using only structural and electronic data on the reactants and products [31]. However, in the transfer of σ^*-d electrons, the correlation with the experimental data suggested the existence of distance-dependent non-adiabatic factors [31]. More importantly, these calculations were consistent with a spin-forbidden factor of approximately 10^{-3} in exchanges at the $Co^{2+/3+}$ center, as observed experimentally by Song et al. [32] and expected from the consistently larger experimental $\Delta S^{\ddagger}$ values of $Co^{2+/3+}$ compounds compared with isostructural $Ru^{2+/3+}$ and $Fe^{2+/3+}$ couples [31]. Spin-forbidden factors of this magnitude in cobalt–amine complexes have also been calculated by several other workers [33–35]. Cross-relations in ET were also addressed with remarkable success, although an empirical parameter, constant for fam-

ilies of reactions, had to be included for strongly exothermic reactions [36]. The same methodology was applied to self-exchanges of organic species with good results [37]. The objectives of the present study of ET reactions between donors and acceptors at restricted distances are as follows:

1. to provide a quantum mechanical treatment for electronic motion which can offer a simple but quantitative account of distance-dependent non-adiabatic factors;
2. to show that the methodology developed by ISM for the calculation of the free energy barriers to nuclear motion in ET reactions can be extended to donors and acceptors in intramolecular systems;
3. to associate the structural and electronic parameters employed in self-exchanges with the treatment of electronic motion, and to calculate long-range intramolecular ET as a function of the distance between donor and acceptor and of the exothermicity of the reactions;
4. to develop a quantitative treatment of the distance-dependent factors empirically estimated in earlier calculations on σ^*-d electron exchanges.

It is a pleasure to contribute this work to the anniversary issue celebrating the 100th volume of the *Journal of Photochemistry and Photobiology A: Chemistry*, in particular because it follows earlier applications of the ISM to chemical reactivity, including photoinduced ET reactions, published in this journal.

2. Theoretical models

The ISM was initially developed [38,39] to calculate the rate constants of atom and group transfer reactions in the gas phase and in solution [40]. Its goal was to obtain a simple analytical method to calculate reaction energy barriers using structural and electronic properties of the reactants and products, the knowledge of the reaction energy and general ideas from transition state theory. In keeping with this goal, a unidimensional reaction coordinate was defined in terms of the distortion of the reactive bonds from their equilibrium positions to their configuration at the transition state, using classical treatment. It was found that these geometric changes in the reactive bonds had to be scaled by the corresponding equilibrium bond lengths. A scaling factor, analogous to that introduced by Pauling in his bond order–bond length relationship, was included in these calculations.

Following successful applications to proton transfer reactions [41–50], ISM was tentatively applied to ET reactions [51–54] with one major conceptual change: the bond order of the reactants was kept constant along the reaction coordinate. This restriction is required by the nature of outer-sphere ET, where no bond breaking–bond forming processes occur. Recently, we undertook a comprehensive study of ET reactions within the framework of the ISM. The first type of reaction to be systematically studied was electron self-exchange in transition metal complexes [31]. The calculated rates were in better agreement with experiment than those calculated by Marcus theory at the same level of sophistication. Non-adiabatic factors were included in σ^*-d electron transfers. This study employed a classical formulation of ISM and the non-adiabatic factors had to be treated empirically. Next, ISM was used to calculate the self-exchange rates of small species ($ClO_2^{-/0}$, $NO_2^{-/0}$, $O_2^{-/0}$) and the cross-reaction ET rates of metal complexes and small species [36]. It was gratifying to see that the parameters employed in self-exchanges could be directly transferred to cross-reactions. For families of very exothermic reactions, a common empirical parameter, related to the reaction dynamics, had to be introduced. Finally, self-exchanges of organic species were treated as adiabatic ET reactions [37]. These reactions could be treated classically and no adjustable parameters had to be included. For long-range ET between organic species, distance-dependent non-adiabatic factors must be included, and a model was introduced to calculate such factors [37].

There are two major differences between ISM and Marcus theory: (1) Marcus theory assumes that the solvent reorganization energy is the dominant contribution to the reaction energy barrier, whereas ISM considers that the contribution of non-specific solvent effects to this barrier is less than 5 kJ mol^{-1}; (2) Marcus theory calculates the internal reorganization energy presuming that the activated complex configuration of a bond involved in the reaction coordinate (l^*) is intermediate between that of its oxidized and reduced forms ($l_{ox} \leq l^* \leq l_{red}$ or $l_{red} \leq l^* \leq l_{ox}$, where l represents the bond length), while ISM predicts that the activated complex configuration corresponds to a stretching of the bonds participating in the reaction coordinate ($l^{\ddagger} \geq l_{red}, l_{ox}$).

The predictions of Marcus theory concerning the effect of the solvent in the ET reaction barrier can be conveniently assessed by analysing the experimental solvent dependence of electron self-exchange rates in systems with one uncharged reactant. Such systems are free from solvent effects in the reaction free energies (ΔG^0) and in the work terms. A most striking example of the (lack of) solvent effects on ET energy barriers is the experimental observation that the self-exchange reactions of alkylhydrazines have nearly the same energy barrier in acetonitrile and in the vapour phase [55], while Marcus theory predicts that, with a distance $r = 700$ pm between the centers of the reactants in the activated complex [56], $\Delta G^{\ddagger}$ in acetonitrile should be larger by 26 kJ mol^{-1} than that in the vapour phase. A survey of electron self-exchange reactions involving transition metal complexes also reveals the magnitude of solvent effects in ET rates. Ferrocene/ferrocenium and cobaltocene/cobaltocenium are predicted (with $r = 760$ pm) to exhibit a 15-fold increase in the rate when the solvent is varied from methanol to benzonitrile or nitrobenzene, but factors of 1.5 increase and 1.2 decrease are observed respectively [57]. The self-exchange rate of tris(hexafluoroacetylacetonato)ruthenium(II/III) should increase by a factor of 8.2 (using $r = 1000$ pm) when the solvent is changed from methanol to nitrobenzene, but only a factor of 4.9 increase is observed [58]. When the solvent is varied from propylene carbonate to benzonitrile, the

exchange rate of bisbiphenylchromium(0/I) should increase by a factor of 3.1 ($r = 1160$ pm) and experimentally it increases by a factor of 2.5 [59]. Apparently, the agreement between Marcus theory predictions and the experimental observations on solvent effects in ET rates improves as the reactants become larger, i.e. as no solvent dependence is predicted. These and other results have led to the recent conclusion that the rates of self-exchange are typically only marginally influenced by changes in solvent identity [60]. If ISM gives a correct description of ET reactions, then it is expected that non-specific solvent effects will lead to 5 kJ mol^{-1} variations in $\Delta G^{\ddagger}$, i.e. that the self-exchange rates should vary by less than a factor of 7.5 at room temperature. This is confirmed by the experimental data.

The new trend emerging in the literature considers that the internal reorganization is the major contributor to the activation energy of many ET reactions, and little room is left for solvent reorganization [61,62]. However, if Marcus theory overestimates the solvent reorganization energy and, in many cases, calculates rate constants in agreement with the experimental values [63,64], such overestimation must be compensated by an underestimation of the internal reorganization energy. Thus we are led to believe that the activated complex configuration corresponds to a larger distortion of the reactant modes than is used in Marcus theory, i.e. $l^{\ddagger} \geq l_{red}, l_{ox}$. This suggests that ISM gives a correct description of the reaction coordinate and prompts us to extend the application of this model to other ET processes.

2.1. Nuclear factors

At its present level of sophistication, ISM treats the nuclear motion classically. The equations that govern the nuclear motion along the reaction coordinate have been discussed elsewhere [31,36,40]. Thus the following presentation of the model for nuclear motion focuses on the concepts involved rather than the derivation of equations. Next, we discuss the quantum mechanical treatment of electronic motion along the reaction coordinate, supplementing earlier applications of ISM which do not offer a quantitative approach to this factor. The combination of a classical treatment of the nuclear motion with a quantum mechanical treatment of the electronic factor results in a semiclassical formulation of ISM. This mixture of classical and quantum arguments may seem to result in a crude model of chemical reactivity. However, like many other hybrid models coexisting in this field, this very mixture of ingredients leads to formulae which can be treated without resorting to adjustable parameters or compromising the physical meaning of the model. The ultimate value of this approach has to be assessed from a comparison between calculated and observed rate constants.

The adiabatic transfer of an electron from a donor to an acceptor will occur every time the configuration and energy of the nuclei in the reactants and products are identical. These are the conditions that determine the nuclear configuration of the transition state in real systems. ISM defines the nuclear reaction coordinate as the sum of the distortion of the molecular bonds from their equilibrium positions towards the transition state configuration

$$d = (l_r^{\ddagger} - l_r) + (l_p^{\ddagger} - l_p) \quad (1)$$

where l_r and l_p are the equilibrium bond lengths of the reactants and products, and provides geometric criteria for their determination. These criteria establish that, when the reaction free energy is close to zero, the variation in each bond length along the reaction coordinate is ruled by its transition state bond order in a manner that can be related to the equation Pauling introduced for stable species

$$\ln n_r^{\ddagger} = -\frac{1}{a}(l_r^{\ddagger} - l_r) \quad (2)$$

where a is a "universal constant". The variation in each bond length is also proportional to the equilibrium length of the bond being distorted. Thus the reaction coordinate is determined by the bond order and equilibrium bond length of each reactive bond. In order to keep the model unidimensional, the contributions of all the reactive bonds are averaged. The resulting expression for the reaction coordinate can be written as

$$d = \frac{a' \ln 2}{n^{\ddagger}}(l_r + l_p) \quad (3)$$

where $n^{\ddagger}$ is the average transition state bond order, l_r and l_p are the average equilibrium bond lengths of the reactants and products and $a' = 0.156$ is a constant analogous to that defined by Pauling.

It is the displacement of the nuclei from their equilibrium positions that leads to the reaction energy barrier. The energy variations involved in the stretching of the bonds are much higher than those associated with other vibrations, and thus only these vibrations will be considered here. In order to obtain analytical solutions to these vibrational modes, each bond is treated as a harmonic oscillator characterized by a force constant. Again, to maintain a unidimensional model, averages for the force constants of the reactive bonds are used. The relations between all the variables involved in our calculations of self-exchange rates are represented in Fig. 1.

The reaction free energy barrier $\Delta G^{\ddagger}$ has to be overcome by the thermal fluctuation of nuclear positions. The process by which nuclei acquire enough energy to overcome this barrier is irrelevant for the calculations provided that the transition state species which start as reactants are in local equilibrium with the reactant states. This is the first of the two fundamental assumptions of transition state theory, and that which makes it a statistical mechanical theory [65]. Consequently, the nuclear barrier crossing problem can be formulated in thermodynamic terms, and free energy plots should be employed to obtain phenomenological ET rate constants [31]. The second assumption of transition state theory is that the molecules with energies equal or larger than $\Delta G^{\ddagger}$ cross the transition state configuration with the fre-

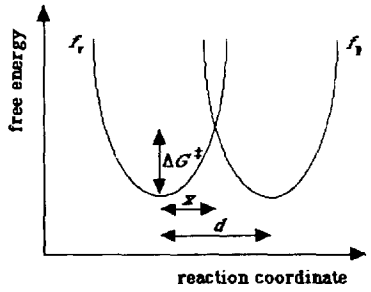

Fig. 1. Free energy profile along the reaction coordinate defined by ISM for an electron self-exchange reaction. Reactants and products are represented by harmonic oscillators with force constants f_r and f_p. The parameter d represents the sum of the bond distortions of the bond lengths of the reactants and products from their equilibrium positions to their transition state configuration.

quency $\nu_n = k_B T/h$, and have unitary probability of yielding products. If these conditions are followed, the adiabatic bimolecular rate constant can be calculated from

$$k_{ad} = \frac{k_B T}{h}(c_0)^{-1} \exp(-\Delta G^{\ddagger}/RT) \quad (4)$$

where c_0 is the standard concentration ($c_0 = 1$ M) and the other symbols have their usual meanings. According to ISM, the rate constants of adiabatic ET with reaction free energies close to zero can be calculated by Eq. (3) and Eq. (4). If the reactive bonds are treated as harmonic oscillators, as shown in Fig. 1, the rate constant calculations only require a knowledge of the average bond lengths, force constants and bond orders of the reactants and products.

For more exothermic reactions, Eq. (3) must be replaced by

$$d = \frac{a'}{2n^{\ddagger}} \ln\left\{\frac{1+\exp(\sqrt{2n^{\ddagger}}\Delta G^0/\lambda)}{1-[1+\exp(\sqrt{2n^{\ddagger}}\Delta G^0/\lambda)]^{-1}}\right\}(l_r + l_p) \quad (5)$$

which introduces an additional parameter λ associated with the dynamics of the reactions. This parameter is not related to the reorganization energy parameter of Marcus theory which is usually represented by the same symbol. It is convenient to discuss in more detail the physical meaning of the new concepts introduced by ISM and translated by $n^{\ddagger}$, a' and λ in Eq. (5).

2.1.1. The nature of the transition state bond order $n^{\ddagger}$

Most frequently, during an electron exchange, the total bond order of two reactants is conserved, although the bond order of each reactant may vary during the course of the reaction. For example, in the self-exchange

$$C_6H_6 + {}^*C_6H_6^- \rightarrow C_6H_6^- + {}^*C_6H_6$$

benzene has a valence bond order of 1.50 and the benzene anion has a bond order of 1.42 (because the extra electron occupies an antibonding orbital), but the average bond order of 1.46 is preserved during the course of the reaction. This type of bonding and antibonding electron counting can be

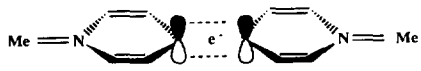

Scheme 1.

used to obtain the bond order of each organic species along the ET reaction coordinate in ET [37]. The transition state bond order $n^{\ddagger}$ of an ET reaction is calculated from the contributions of the two reactants

$$\frac{1}{n^{\ddagger}} = \frac{1}{2n_1^{\ddagger}} + \frac{1}{2n_2^{\ddagger}} \quad (6)$$

The values of $n^{\ddagger}$ for ET involving transition metal complexes with saturated ligands, such as H_2O or NH_3, are equally simple to calculate, because it has been shown that the metal–ligand bonds can be regarded as single bonds [31,36]. Only Ru and presumably Os complexes were found to have increased equilibrium bond orders due to back-bonding. However, transition metal complexes with aromatic ligands, such as bipyridyl or pyridine, were shown to have $n^{\ddagger}$ values that exceeded the equilibrium bond orders [31,36]. This can be explained by considering that the p orbitals of the ligands may interact to accommodate the electron being transferred, in a manner related to inner-sphere processes, leading to an increased value of $n^{\ddagger}$ (Scheme 1). Such increased values of $n^{\ddagger}$ correspond to a high resonance energy at the crossing point of the reactant and product potential energy curves. This interaction leads to metal-to-ligand bonds with double bond character, and thus $n^{\ddagger} = 2$.

2.1.2. The nature of the constant a'

The constant $a' = 0.156$ is a dimensionless proportionality constant between the transition state bond orders and the corresponding reduced bond distortions, which are given by the sum of the distortions of the reactant and product bonds from their equilibrium lengths to the transition state configuration scaled by the equilibrium bond lengths

$$\eta = \frac{(l_r^{\ddagger} - l_{r,eq}) + (l_p^{\ddagger} - l_{p,eq})}{l_{r,eq} + l_{p,eq}} \quad (7)$$

The value of a' was obtained [38] from a correlation between η and $1/n^{\ddagger}$ for atom transfer reactions of the type $H + H_2$, $Cl + H_2$ and $H + I_2$, and was found to lead to good agreement between the transition state configurations calculated by ISM and ab initio methods for the reactions $H + H_2 \rightarrow H_2 + H$, $H_2 + Cl \rightarrow H + HCl$ and $H + HF \rightarrow H_2 + F$. This scaling factor seems to be a universal scaling factor for ISM calculations, because it has been successfully used as a constant for a large diversity of reactions: atom and proton transfer reactions, ET reactions, cation–anion recombinations, etc. It is not treated as an adjustable parameter.

2.1.3. The nature of the dynamic parameter λ

The parameter λ has been related to the amount of vibrational energy released in the nascent products. It increases with the capacity of the activated complex to convert ΔG^0

into translational and/or vibrational energy of the non-reactive modes of the products. For reactions in solution, it is treated as an adjustable parameter, but its effect on the calculated rate constants is only significant for reactions with $\Delta G^0 < -50$ kJ mol^{-1}. Furthermore, the qualitative dependence of λ on several reaction conditions can be predicted, because λ is expected to be low when $\Delta S^{\ddagger}$ is low (tight transition state) and high when $\Delta S^{\ddagger}$ is high (loose transition state). For example, λ increases with an increase in the solvent polarity or the rigidity of the medium. This parameter is constant for a family of structurally related reactants undergoing the same type of reaction under the same conditions. It scales the impact of ΔG^0 on d.

The free energy of activation of self-exchange reactions ($\Delta G^0 = 0$) can be calculated with d given by Eq. (3) and the relations expressed in Fig. 1

$$\Delta G^{\ddagger} = \frac{1}{2} f_r \left(\frac{d}{2}\right)^2 \tag{8}$$

where f_r is the force constant of the reactants. Such calculations do not require adjustable parameters and can be designated as absolute rate calculations. When $\Delta G^0 \neq 0$, $\Delta G^{\ddagger}$ must be calculated from the relations

$$\frac{1}{2} f_r x^2 = \frac{1}{2} f_p (d-x)^2 + \Delta G^0 \tag{9a}$$

$$\Delta G^{\ddagger} = \frac{1}{2} f_r x^2 \tag{9b}$$

where x is the average bond extension of the reactants from their equilibrium position to their configuration at the transition state and d is given by Eq. (5). In this case, λ must be estimated and its value becomes relevant when $\Delta G^0 < -50$ kJ mol^{-1}.

2.2. Electronic factors

The importance of the medium separating the electron donor and acceptor in the stabilization of the energy of the electron during the ET process has been recognized by many workers. For example, Mann and Kuhn [4] proposed that fatty acids stabilize the electron energy by an empirically obtained constant factor of 2.25 eV, independent of the nature of the donor and acceptor, and compared this factor with the electron affinity of rigid organic solutions determined by Johnson and Albrecht [66]. What these workers actually measured was the photoconductivity of *N,N,N′N′*-tetramethylparaphenylenediamine (TMPPD) in 3-methylpentane (3MP) at 77 K, and concluded that the ionization potential (I_P) of TMPPD decreases from $I_{P(gas)} = 6.6$ eV in the gas phase to $I_{P(sol)} = 5.9$ eV in rigid 3MP solution. The ionization potential of a solute has been expressed [67] as $I_{P(sol)} = I_{P(gas)} + P_+ + V_0$, where P_+ is the adiabatic polarization energy of the medium by the positive ion and V_0 is the energy of the electronic conduction level in the dielectric relative to the vacuum. V_0 for non-polar hydrocarbon liquids at room temperature tends to range from +0.2 to −0.6 eV [68]. There are two contributions to V_0: short-range repulsive forces and the polarization energy due to long-range interactions of the electron with the fluid. The former serves essentially to confine the electron to limited regions and can be expressed in terms of a zero-point kinetic energy [69]. The latter should have a functional form similar to that of the electronic polarization energy of the positive ion which, for liquids, Holroyd [70] has suggested may be represented by the Born charging energy, i.e. has a reciprocal dependence on the square of the refractive index of the liquid. The assumption that the stabilization of the energy of the electron during the tunneling process is only a function of the properties of the dielectric is in conflict with the experimental data. Krongauz [12] clearly showed that tunneling barrier heights calculated from the medium properties alone cannot account for the observed ET distance dependence, either using a tunneling or superexchange model. We believe that the failure of this model when applied to ET processes is related to its picture of a localized electron, which is not applicable to a tunneling process.

Our approach to the distance-dependent electronic factors in ET reactions is to consider that the electron has to tunnel from the donor to the acceptor through a potential energy barrier of variable length. More specifically, the energy variation along the electronic coordinate of a long-range ET can be simulated by representing the donor by a potential energy well containing the electron and the intervening medium between the donor and acceptor by a rectangular barrier. The height of this barrier is given by the energy of the electron in the medium relative to its energy in the donor, Φ. The width of the tunneling barrier is determined by the edge-to-edge distance between the donor and acceptor, R_e. This simple model is pictured in Fig. 2. The Wentzel–Kramers–Brillouin (WKB) solution for the probability of a particle to escape from a potential well through the type of potential energy curve illustrated in Fig. 2 is well known [71]

$$\chi_R = \exp\left[-\frac{2\sqrt{2m_e\Phi}}{\hbar} R_e\right] \tag{10}$$

The distance dependence of ET can be associated with χ_R, giving for the tunneling decay coefficient

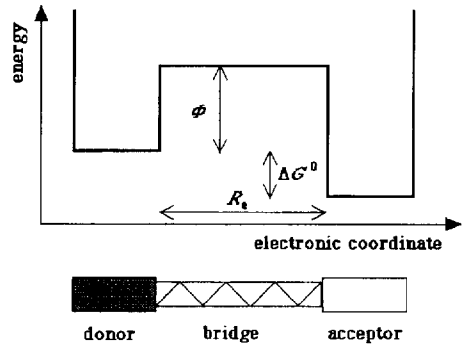

Fig. 2. Schematic representation of the electron tunneling barrier separating the reactant and product potential energy wells in a rigid system.

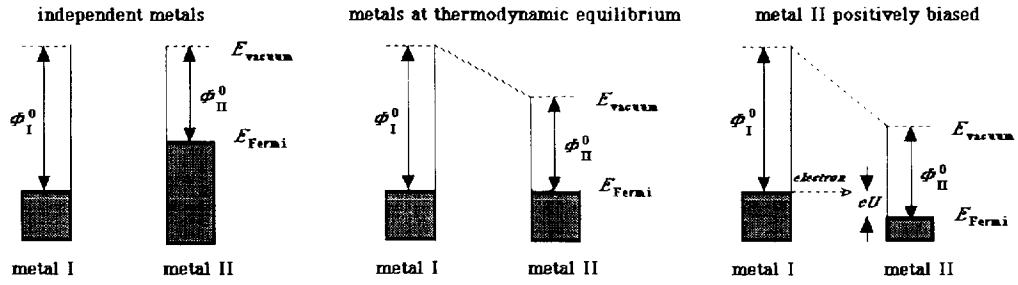

Fig. 3. Electronic energy levels of metals. For independent metals, the vacuum levels are equal and the Fermi levels lie below the vacuum levels by their respective work functions. When the metals are at equilibrium and separated by a small gap, the energies of the Fermi levels are equalized. If a positive voltage U is applied to metal II, its energy shifts downwards by the amount eU, and electrons will flow from metal I to metal II.

$$\beta_{calc} = \frac{2\sqrt{2m_e\Phi}}{\hbar} = 1.025\sqrt{\Phi} \quad (11)$$

With the constant used in this equation, when Φ is expressed in electronvolts, β_{calc} will be expressed in $Å^{-1}$.

Following this model, the determination of the distance dependence of ET becomes simply a matter of calculating the height of the tunneling barrier. In the limiting case of an electron being transferred between two metals through a vacuum, as observed in scanning tunneling microscopy (STM) [72,73], the tunneling barrier is trapezoidal. For typical values of the electronic work functions of the metals involved in these processes, Φ can be calculated as the average of the work functions of both metals (Fig. 3). If an intervening medium is placed between the metals, a stabilization of the virtual energy of the electron in that region will occur, and a reduction in β_{calc} should be observed. When the lowest energy conduction band of the intervening medium is of much higher energy than the initial energy of the electron, this medium can be treated as a dielectric. The stabilization of charge separation by dielectrics is well known from electrostatics. If the charges produced in the detachment of an electron from a molecule can be treated as stationary, the Coulomb potential experienced by the electron at a given distance from the cation in the vacuum (Φ_0), relative to the potential (Φ) experienced at the same distance when the system is immersed in a medium of permittivity ε, will be

$$\frac{\Phi_0}{\Phi} = \varepsilon_r \quad (12)$$

where ε_r is the relative permittivity (or static dielectric constant) of the medium.

However, the electron cannot be treated as a stationary charge in ET reactions. The frequency of the movement of an electron singly occupying an antibonding delocalized molecular orbital of the donor can be estimated from the zero-point energy of a particle in a unidimensional potential well of infinite walls (E), and the relation $E = h\nu$, giving

$$\nu_{el} = \frac{h}{8m_e r_D^2} \quad (13)$$

where r_D is the effective length of the lowest energy antibonding molecular orbital of the donor, measured along the donor–acceptor axis, and m_e is the mass of the electron at rest. Typical conjugated π molecular orbitals of electron donors have sizes from 0.9 nm down to 0.3 nm. For such r_D values, Eq. (13) leads to electronic frequencies in the range 10^{14}–10^{15} s^{-1}, in excellent agreement with the electronic frequency factors employed by Miller and coworkers for similar processes [11,74]. At such high frequencies, only the electronic component of the polarizability of the molecules constituting the intervening medium can contribute to its relative permittivity. The orientation and distortion polarizations cannot contribute to the stabilization of charge separation in such fast processes. It follows from the Maxwell equations that the relative permittivity at a specified frequency is related to the square of the refractive index at that frequency

$$\varepsilon_r = (n_r)^2 \quad (14)$$

The frequency of the yellow light from sodium vapour (5.0×10^{14} s^{-1}), most often used to determine the refractive index of substances n_D, is similar to the high frequencies of electronic motion in molecules. Therefore the static dielectric constant employed in Eq. (12) must be replaced by the optical dielectric constant or by the experimentally determined value of $(n_D)^2$, which is equivalent in the relevant frequency range. Taking into consideration the effect of the dielectric in long-range ET, the tunneling barrier height (Φ) can now be calculated as the potential energy of the highest energy electron in the electron donor relative to the energy of the electron at rest in the vacuum (Φ_0), corrected by the optical dielectric constant of the medium

$$\Phi = \frac{\Phi_0}{(n_D)^2} \quad (15)$$

The scaling of the tunneling barrier height by $(n_D)^2$ is not unexpected in view of the definition of the refractive index of a medium

$$n_D = c/\nu \quad (16)$$

where c is the speed of light in the vacuum and ν is its speed in the medium. Given the wave-like behavior of particles, this is very suggestive of

$$E_{k(medium)} = E_{k(vacuum)}/n_D^2 \quad (17)$$

where E_k represents the kinetic energy of the electron in the tunneling process.

Eq. (11) and Eq. (15) provide the framework to calculate the tunneling decay coefficients of long-range ET without explicit consideration of the molecular structure of the intervening medium. Therefore their great simplicity should be matched by their applicability to a wide range of systems. Actually, the experimental refractive index accounts for the molecular structure of the medium, and the fundamental approximation of this model is to consider that the interaction of the electron with the dielectric in its tunneling path parallels the interaction of electromagnetic radiation when it propagates through the dielectric. In view of their similar frequencies and wave-like behavior in the tunneling phenomenon, this seems to be a reasonable model.

The calculation of the non-adiabatic factor at contact (χ_0), i.e. when $R_e = 0$, is not a concern of this work. For the reasons stated previously, we will take $\chi_0 = 10^{-3}$ for spin-forbidden ET at cobalt–ammine redox centers. There is another system considered in this work for which we made $\chi_0 < 1$. In this system, the reactive state is in equilibrium with non-reactive states, and χ_0 reflects the fraction of reactive states populated.

In our earlier calculations on adiabatic bimolecular intermolecular ET rates, the pre-exponential factor was taken from transition state theory (Eq. (4)). In non-adiabatic intramolecular ET, special attention must be given to the choice of an appropriate pre-exponential factor. According to the model pictured in Fig. 2, the impact of the electron in the tunneling barrier occurs with a frequency ν_{el}, but the probability of escape of the electron is given by $\chi_0\chi_R$. Thus the reactive electronic frequency in ET is $\chi_0\chi_R\nu_{el}$. Given the small range of sizes of the electron donors addressed in this study, we make $\nu_{el} = 5 \times 10^{14}$ s^{-1} for all the intramolecular reactions presented here.

2.3. Calculation of ET rate constants

We have now concluded the formulation needed to calculate non-adiabatic intramolecular ET rates. Such non-adiabatic rates can be calculated from

$$k_{nad} = \chi_0\chi_R\nu_{el} \exp(-\Delta G^{\ddagger}/RT) \quad (18)$$

When ΔG^0 is close to zero, the reaction free energy barrier can be obtained from Eq. (3) and Eq. (8), and the calculation of k_{nad} does not require the adjustment of any parameters to the kinetic data. We refer to such semiclassical calculations as absolute rate constant calculations. For significantly exothermic reactions, $\Delta G^{\ddagger}$ must be calculated using Eq. (5) and Eq. (9a) and Eq. (9b); at this level of sophistication of the model, for such exothermic reactions, one adjustable parameter (λ) is involved.

The following part of this work presents two types of calculation. First, we test the validity of our tunneling model by applying Eq. (11) and Eq. (15) to calculate the tunneling decay coefficients of distance-dependent ET in widely different systems. Then we calculate the non-adiabatic ET rate constants. Such rates are calculated according to the following procedure.

1. The ET reactive center of each reactant is identified. For a transition metal complex, it is usually composed of metal–ligand bonds. For an organic species, it involves the conjugated system, except when the electron is preferentially localized elsewhere, e.g. in the nitro group of nitrobenzene.
2. The experimental bond lengths of the reactive bonds of each reactant are taken from the literature. The model is not very sensitive to small variations in these bond lengths. These bond lengths are averaged to obtain a unidimensional reaction coordinate.
3. The diagonal stretching force constants of the reactive bonds of each reactant are taken from the literature. For transition metal complexes, where the oscillators are independent, the effective force constant is calculated as $f_{eff}^2 = \Sigma f_i^2$. For organic molecules, the effective force constant is the average of the force constants of the reactive bonds.
4. The valence bond order of each reactant is the average of the bond orders of its reactive bonds. The ET transition state bond order $n^{\ddagger}$ is given by Eq. (6). As mentioned above, transition metal complexes with aromatic ligands may have enhanced values of $n^{\ddagger}$ relative to the valence bond order of the reactants.
5. With the values of the effective bond lengths and $n^{\ddagger}$ determined above, Eq. (5) can be used to obtain the reaction coordinate d. When $|\Delta G^0| < 50$ kJ mol^{-1}, absolute calculations can be performed using, for example, $\lambda = 250$ kJ mol^{-1}, because the value of d is not very sensitive to the value of λ.
6. The free energy barrier $\Delta G^{\ddagger}$ is calculated with Eq. (8) (self-exchange) or Eq. (9a) and Eq. (9b) (asymmetric ET).
7. Distance-dependent non-adiabatic factors are calculated with Eq. (10) and Eq. (15), where Φ_0 is the energy of the donor relative to the vacuum and n_D is the refractive index of the medium separating the donor and acceptor.
8. The rate of non-adiabatic intramolecular ET between donor and acceptor separated by a rigid spacer is calculated with Eq. (18). For simplicity, the electronic frequency is taken as approximately constant and equal to $\nu_{el} = 5 \times 10^{14}$ s^{-1}.

3. Results

The calculation of tunneling decay coefficients according to Eq. (11) and Eq. (15) requires a knowledge of the absolute potential of the electron donor and the refractive index of the intervening medium. The energy of the electron in the donor (D^-) relative to its energy in vacuum can be estimated from the standard electrochemical reduction potential of the donor relative to a given reference electrode and the absolute potential of that reference electrode

$$\Phi^0(D^-) = E^0(D/D^-) + \Phi^0(\text{ref}) \quad (19)$$

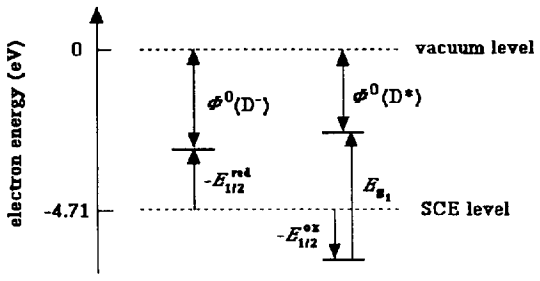

Fig. 4. Schematic representation of the energy of an electron in a reduced electron donor (D^-) and in an electronically excited donor (D^*) relative to its energy in vacuum and in SCE.

If the reaction is reversible, the standard potential E^0 may be replaced by the polarographic half-wave potential $E_{1/2}$ with an error smaller than 10 mV [75]. In photoinduced ET, the energy of the excited electron in the donor (D^*) can be obtained from the standard electrochemical oxidation potential of the donor relative to a given reference electrode, the excited state energy of the donor and the absolute potential of the reference electrode

$$\Phi^0(D^*) = E^0(D/D^+) + E^* + \Phi^0(\text{ref}) \quad (20)$$

where E^* can either be the singlet (E_S) or triplet (E_T) excited state energy. These relations are illustrated in Fig. 4. The reference electrodes considered in these calculations are the normal hydrogen electrode in water ($\Phi^0(\text{NHE}) = 4.44$ eV [76]) and the standard calomel electrode ($\Phi^0(\text{SCE}) = 4.71$ eV [77]).

The energy of an electron in a metal relative to its energy in vacuum is given by the electron work function of the metal, Φ^0_M. In order for the electron to tunnel from one metal to another, a bias voltage (U) must be applied to the system (Fig. 3). When a positive bias is applied to metal II ($U > 0$), its energy is lowered by eU, where e is the charge of the electron, and the electrons will tunnel from the Fermi level of metal I to metal II. The applied voltage should also lower the tunneling barrier. This is not explicitly accounted for in our calculations because we consider only systems with low bias voltages. Under this condition and for typical electronic functions of the metals, the tunneling barrier between two metals separated by a vacuum can be approximated by

$$\Phi^0(M) = \frac{\Phi^0_{M_I} + \Phi^0_{M_{II}}}{2} \quad (21)$$

In an analogous manner, the energy of an electron in equilibrium between an electroactive center and an electrode can be related to its energy in vacuum by

$$\Phi^0(E) = \frac{\Phi^0_{M_I} + \Phi^0(D)}{2} \quad (22)$$

as illustrated in Fig. 5. In order for an electron to be transferred, an electrode overpotential η must be applied to the system. This overpotential will decrease the height of the tunneling barrier by approximately $|\eta|/2$. More exact formulae for this effect were given by Mann and Kuhn [4]. For typical values of the energy of a transferable electron in an electroactive center (4–5 eV) and for the work functions of the most popular metal electrodes (Au, Pt, Ag), overpotentials smaller than 1 V lead to modest decreases in the tunneling coefficient. For example, taking $\Phi^0(D) = 4.5$ eV, $\Phi^0(M_I) = 5.0$ eV and $(n_D)^2 = 2$, we obtain $\beta_{calc} = 1.58$ Å^{-1} in the absence of overpotential and $\beta_{calc} = 1.49$ Å^{-1} when $\eta = 1$ V is applied. Such small variations in the tunneling coefficient have been observed experimentally [78].

The barrier for ET between two metals may be changed by the existence of image forces. The effect of the image force between two metals is to reduce the area of the potential barrier between them by rounding off the corners and reducing the thickness of the barrier. Simons [79] has shown that the value of the image potential at the middle of the separation between the two electrodes is given by

$$V_i = -e^2 \ln 2/(2\pi\varepsilon R_e) \quad (23)$$

When the separation between the two electrodes is $R_e = 3$ Å and $\varepsilon = 1.88$ as in n-hexane, the effect of the image potential is to reduce the tunneling barrier height by 0.28 eV. If the distance increases to 15 Å, the reduction of the barrier is only 0.056 eV. All ET between metals considered in this work involves $R_e > 15$ Å, and thus image force corrections are not expected to be significant.

In order to correct the tunneling barrier measured relative to vacuum for the effect of the dielectric (Eq. (15)), we take the refractive index of the bridge as that of the molecule that would be obtained if donor and acceptor were replaced by hydrogen atoms.

In Table 3, we present the experimental tunneling decay coefficients (β_{exp}) of a large number and variety of systems. The criterion used in the selection of these data was that the electron donor and acceptor had to be kept at restricted distances during the ET process. We considered that the polymethylene chains used in intramolecular electrochemical ET across $SH(CH_2)_nR$ bridges are tilted with respect to the surface normal by an angle of 30° [16]. With the exception of the systems using more than three proline units as bridges, which were not included for the reasons addressed below, the experimental values range from 0.9 to 2.3 Å^{-1}. In the same

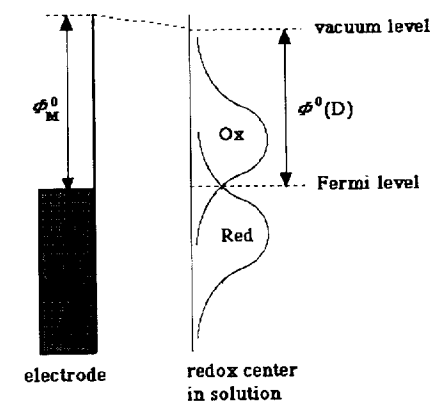

Fig. 5. Electronic energy levels in an electrode in equilibrium with a redox pair in solution.

Table 1
Electrochemical potentials, singlet excited state energies of electron donors and tunneling decay coefficients in intramolecular ET and in ET in rigid matrices [a]

Donor	Spacer	T (K)	Solvent	$E^{red}_{1/2}$ or $E^{ox}_{1/2}$ (eV)	E_{S_1} (eV)	Φ^0 [b] (eV)	n_D	β_{calc} ($Å^{-1}$)	β_{exp} ($Å^{-1}$)	Reference [c]
Biphenyl$^-$	Cyclohexane to steroid	296	THF	−2.58 [d]		2.13	1.41	1.06	1.12	[13]
Biphenyl$^-$	Cubyl	296	THF	−2.58 [d]		2.13	1.41	1.06	0.94 [e]	[80]
Dimethoxynaphthalene*	Polynorbornyl	297	THF	1.1	3.78	2.03	1.41	1.04	0.96	[81]
[Ru(bpy)$_3^{2+}$]*	*n*-Alkyl	296	Acetonitrile	1.22	2.08	3.85	1.41	1.43	1.38	[82]
ZnTTP*	Oligospirocyclic	Room	Acetonitrile	0.75	2.04	3.42	1.41	1.34	1.1	[83]
ZnPAP*	Bicyclo[2.2.2]octyl	298	Acetonitrile	0.68 [f]	2.14 [f]	3.25	1.41	1.31	1.4 [e]	[84]
ZnPAP*	Polyphenylene	Room		0.68 [f]	2.14 [f]	3.25	1.41	1.31	1.20 [g]	[85]
[Ru(Me$_4$phen)$_3^{2+}$]*	Glycerol	250	Glycerol			3.75 [h]	1.5	1.32	1.4	[86]
Biphenyl$^-$	Ethanol	77	Ethanol			1.6 [i]	1.456	0.89	1.06	[87]
2-Ethylanthraquinone$^-$	MTHF	77	MTHF			4.02	1.51	1.36	1.42	[12]
9-Fluorenone$^-$	MTHF	77	MTHF			3.84	1.51	1.33	1.24	[12]
Acridine$^-$	MTHF	77	MTHF			3.55	1.51	1.28	1.22	[12]
Fluoranthene$^-$	MTHF	77	MTHF			3.40	1.51	1.25	1.38	[12]
Pyrene$^-$	MTHF	77	MTHF			3.05	1.51	1.19	1.12	[12]
Biphenylene$^-$	MTHF	77	MTHF			2.90	1.51	1.16	1.26	[12]
Biphenyl$^-$	MTHF	77	MTHF			2.56	1.51	1.08	1.20	[12]
Triptycene$^-$	MTHF	77	MTHF			1.87	1.51	0.93	1.10	[12]
e$^-$(s)	Aqueous NaOH (10 M)	77	Aqueous NaOH			1.1 [j]	1.43	0.75	0.91	[88]

[a] Electrochemical potentials measured against SCE; bpy, 2,2′-bipyridyl; TTP, tetratolylporphyrin; PAP, meso-phenyloctaalkylporphyrin; phen, 1,10-phenanthroline.
[b] Calculated from the electrochemical reduction potential or electrochemical oxidation potential and excitation energy, unless taken from the literature.
[c] References to β_{exp} estimated from edge-to-edge distances, unless otherwise noted; the same reference also applies to $E^{ox}_{1/2}$, E_{S_1} and Φ^0, unless otherwise noted.
[d] Ref. [75].
[e] From the center-to-center distance between donor and acceptor.
[f] Ref. [89].
[g] Recalculated distance dependence using only C–C distances between aromatic rings.
[h] From the free energy of ET to methylviologen in Ref. [90] and the reduction potential of methylviologen in Ref. [82].
[i] Ref. [10].
[j] Ref. [91].

Table 2
Tunneling decay coefficients of a vacuum–tunnel junction and of ET across monolayers in metal–dielectric–metal junctions and metal–dielectric–electroactive center [a]

Metal I	Spacer	Metal II or electroactive center	T (K)	Solvent	Φ_I^0 (eV)	Φ_{II}^0 or $\Phi^0(D)$ [b] (eV)	n_D	β_{calc} [c] ($Å^{-1}$)	β_{exp} ($Å^{-1}$)	Reference [d]
Pt	Vacuum	W	Room		5.03	4.55	1.00	2.24	2.17	[72,73]
Al	Perfluorinated fatty acids (adsorbed)	Al	77		4.20	4.20	1.29 [e]	1.63	2.3	[92]
Au	Fatty acid (LB)	Al	293		4.80	4.20	1.43 [f]	1.50	1.6	[93]
Hg	Fatty acid (LB)	Al	293		4.50	4.20	1.43 [f]	1.49	1.49	[4]
Al	Fatty acids (LB)	Al	293		4.20	4.20	1.43 [f]	1.47	1.6	[93,94]
Al	Fatty acids (adsorbed)	Al	77				1.43 [f]	1.47	1.5	[92]
Mg	Fatty acids (LB)	Al	293		3.65	4.20	1.43 [f]	1.42	1.1	[93]
Pt	py-$\{CH_2\}_{0,2,3}$-	$pyOs^{II}(bpy)_2Cl$	298	THF	5.03	5.0	1.355 [g]	1.69	1.62	[17]
Au	SR-$\{CH_2\}_{1-4}$-	$COOCo^{III}(NH_3)_5$	Room	Water	4.80	4.4	1.50 [h]	1.47	1.61	[15]
Au	SH-$\{CH_2\}_{8,12,16}$-	$COOCpFe^{II}Cp$	130–150	EtCl/PrCN	4.80	4.8	1.63 [i]	1.38	0.96 [j]	[18]
Au	SH-$\{CH_2\}_{8,12,16}$-	$COOCpFe^{II}Cp$	130–150	EtCl/PrCN	4.80	4.8	1.63 [i]	1.38	1.31 [k]	[18]
Au	SH-$\{CH_2\}_{10,11,15}$-	$CONHCH_2pyRu^{II}(NH_3)_5$	295	Water	4.80	4.7	1.62 [l]	1.38	0.98 [j]	[95]

[a] Physical or electrochemical work functions (Φ_I^0 and Φ_{II}^0) for polycrystalline surfaces of metals from Ref. [96].
[b] Absolute electrode potentials.
[c] The tunneling barrier heights were calculated using Eqs. (21) and Eq. (15) or Eq. (22) and Eq. (15).
[d] References to β_{exp}.
[e] Ref. [97].
[f] From stearic acid.
[g] From *n*-pentane.
[h] From mercaptoacetic acid.
[i] From mercaptoacetic acid, corrected for the increase in chain length, replacement of an acid by an amide and lower temperature.
[j] From the exponential dependence of the rate constants on the alkane chain length.
[k] From the exponential dependence of the pre-exponential factor on the alkane chain length.
[l] From mercaptoacetic acid, corrected for the increase in chain length and replacement of an acid by an amide.

tables, we also present the tunneling decay coefficients (β_{calc}) calculated according to Eq. (11) and Eq. (15) associated with Eq. (19), Eq. (20), Eq. (21) or Eq. (22). The calculated values are in the range 0.8–2.2 Å^{-1}. The correlation between the calculated and experimental values is presented in Fig. 6. The point representing adsorbed perfluorinated fatty acids as bridges (■) was not included in the correlation. For the reasons addressed in Section 4, this figure does not include the data obtained from the exponential dependence of the electrochemical transfer rates on the bridge lengths if these bridges are longer than 10 Å; instead, for these systems, the purely electronic factor of the distance dependence was included in the correlation when available.

Calculations of intramolecular ET rate constants can be made using the data presented in Table 4 and Table 5. With the exception of the parameter χ_0, which is smaller than unity for spin-forbidden exchanges and when the equilibrium constant between reactive and non-reactive states is smaller than unity, and λ, which is only relevant for very exothermic reactions, all the other parameters were taken from fields outside chemical kinetics. Thus for spin-allowed exchanges with $|\Delta G^0| < 60$ kJ mol^{-1}, absolute rate constants can be calculated. The calculations presented in Fig. 7(a), Fig. 8(a) and Fig. 9 fall into this category. The calculations shown in Fig. 10 refer to a system in which $\Delta G^0 < -100$ kJ mol^{-1} which is appreciably sensitive to the value of λ. However, the calculations for the system $(NH_3)_5Os$-py-{pro}-$ORu(NH_3)_5$, shown in Fig. 11(a), can also be considered as absolute values.

Fig. 7(b), Fig. 8(b) and Fig. 11(b) illustrate the free energy dependence of the intramolecular ET rates, and compare the experimental (points) and calculated (lines) values. Given the nature of the dependence investigated in these calculations, the parameter λ had to be adjusted for each family of reactions. However, this is the only adjustable parameter employed in our calculations of ET reactions.

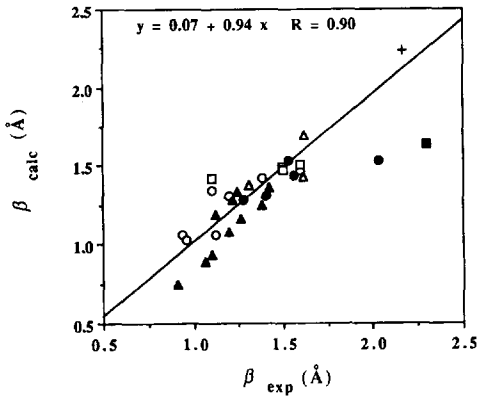

Fig. 6. Correlation between calculated and experimental tunneling decay coefficients using the data from Tables 1–3. The line was obtained by linear regression, excluding the points representing ET through perfluorinated fatty acids (■) and through prolines (●); the correlation coefficient of this line is 0.90; its slope is 0.9 and the y intercept is 0.07. This correlation includes ET through vacuum (+), intramolecular ET in solution (○), ET in rigid media (▲), unimolecular electrochemical ET (△) and ET across adsorbed monolayers (□).

4. Discussion

The analysis of Fig. 6 reveals that the tunneling model employed to calculate the distance dependence of ET in a large number and diversity of systems gives a good account of the absolute and relative values of the tunneling decay coefficients. Only a few systems merit detailed discussion.

Table 3
Reduction potentials of electron donors and tunneling decay coefficients in intramolecular ET through prolines [a]

Donor	Spacer	Acceptor	$E^{redb}_{1/2}$ (eV)	Φ^{pc} (eV)	n_D [d]	β_{calc} (Å^{-1})	β_{exp}(i) [e] (Å^{-1})	β_{el}(i) [e] (Å^{-1})	β_{exp}(f) [f] (Å^{-1})	β_{el}(f) [f] (Å^{-1})
$(NH_3)_5Os^{II/III}$-py [g]	{proline}$_{0-4}$	RO-$Co^{III}(NH_3)_5$	−0.30 [h]	4.14	1.36	1.53	2.03	1.34		
$(NH_3)_5Os^{II/III}$-py [i]	{proline}$_{0-4}$	RO-$Ru^{III}(NH_3)_5$	−0.30 [h]	4.14	1.36	1.53	1.53	0.67		
$(bpy)_2Ru^{II}$-bpy* [j]	{proline}$_{0-3}$	RO-$Co^{III}(NH_3)_5$	−0.8	3.64	1.36	1.44	1.56	0.67		
$(bpy)_2Ru^{II}$-bpy$^-$ [k]	{proline}$_{1-6}$	RO-$Co^{III}(NH_3)_5$	−1.2	3.24	1.44	1.28	1.28		0.29	0.46
$(bpy)_2Ru^{II}$-bpy$^-$ [l]	{proline}$_{6,7,9}$	py-$Ru^{III}(NH_3)_5$	−1.2						0.19	0.50

[a] The tunneling decay coefficients were obtained either from the room temperature ln k vs. distance dependence (β_{exp}) or from the $\Delta S^{\ddagger}/R$ vs. distance dependence (β_{el}); only the slopes of the plots with correlation coefficients larger than 0.97 are presented.
[b] Electrochemical potentials measured against NHE.
[c] Calculated from $E^{red}_{1/2}$ and Φ^0(NHE) = 4.44 V.
[d] From methylacetate when {proline}$_{0-4}$ and from *N*,*N*-dimethylacetamide when {proline}$_{1-6}$.
[e] Assuming that a linear correlation exists within the first three members of each series.
[f] Assuming that a linear correlation exists within the last three members of each series.
[g] Ref. [98].
[h] $E^{red}_{1/2} = 0.2$ V when {proline}$_0$.
[i] Ref. [99].
[j] Ref. [100].
[k] Ref. [101].
[l] Ref. [102].

Table 4
Parameters outside the field of chemical kinetics employed in the calculations of the intramolecular ET rates

Reactant	$n^{\ddagger}$ [a]	l_{ox} [b] (pm)	l_{red} [b] (pm)	f_{ox} [b] (J mol^{-1} pm^{-2})	f_{red} [b] (J mol^{-1} pm^{-2})
Naphthalene$^{0/-}$	1.43	139.8 [c]		381 [c]	
Biphenyl$^{0/-}$	1.44	139.9 [d]		372 [e]	
Anthraquinone$^{0/-}$	1.44	137.5 [f]	138.5 [g]	449 [h]	429 [i]
2,2'-Bipyridine	1.44	138.8 [j]		376 [k]	
Methylviologen	1.46	137.5 [l]		401 [l]	
Dicyanoethylene$^{0/-}$	1.95	130.6 [m]	130.1 [m]	617 [n]	585 [n]
Pyridine$^{0/-}$	1.46	137.6 [o]		422 [p]	
ZnTTP	2.00	203 [q]		116 [r]	
$Ru(bpy)_3^{3+/2+}$	2.00	205.6 [s]	203.4 [s]	323 [s]	323 [s]
$Co(NH_3)_5OCOR^{3+/2+}$	1.00	195 [s]	217 [s]	363 [s]	195 [s]
$Ru(NH_3)_5OCOR^{3+/2+}$	1.38 [s]	211 [s]	214 [s]	384 [s]	298 [s]

[a] Average valence bond order of oxidized and reduced species; for organic species, it was calculated as described in the text for benzene$^{0/-}$; for ZnTTP and $Ru(bpy)_3^{2+/3+}$, the transition state bond order was set equal to two for the reasons discussed in the text and illustrated in Scheme 1; for the other transition metal complexes, it was taken as the average of published bond orders of analogous complexes [36].
[b] Organic species: average bond lengths or force constants of all but the C–H bonds, which are not expected to contribute to the reaction coordinate; metal complexes: calculated as described in Ref. [36].
[c] Ref. [103].
[d] Ref. [104].
[e] Ref. [105].
[f] Ref. [106].
[g] Calculated with GAMESS under the ROHF approximation according to Ref. [107].
[h] Ref. [108].
[i] Estimated from the ratio of the frequencies of the neutral and anionic species in Ref. [109].
[j] Ref. [110].
[k] Ref. [111].
[l] Ref. [112].
[m] Estimated from tetracyanoethylene in Ref. [113].
[n] Estimated from tetracyanoethylene in Ref. [114].
[o] Ref. [115].
[p] Ref. [116].
[q] Ref. [117].
[r] Zn–N force constant estimated from the ratio of M–N frequencies in low-spin complexes of $Zn(bpy)_3^{2+}$ and $Fe(phen)_3^{2+}$ in Ref. [118], and then multiplied by $\sqrt{4}$ according to Ref. [31].
[s] From data in Ref. [31]; when different ligands are coordinated with the metal ion, the parameters shown are weighted averages of those of the bonds involved.

The electric conduction at 77 K in Al–adsorbed monolayer–Al junctions, when the monolayer is made of a short chain of perfluorinated fatty acids (seven to ten carbon atom chain), seems to have an extremely high distance dependence. Our tunneling model predicts that perfluorinated hydrocarbon chains will give the largest β_{calc} values for a given barrier height, because they have the lowest refractive indices of organic polymers [97]. However, the reported value of β_{exp} for this system is higher than that expected for ET through a vacuum with the same barrier height. Thus either the experimental value is in error or a different mechanism is operating in this system. We are not aware of other measurements of the distance dependence of ET rates across perfluorinated hydrocarbons, but it would be of interest to verify whether such systems exhibit very large β_{exp} values.

The distance dependence of ET rates in electrochemical experiments also requires special attention. The β_{exp} values reported for apparently similar systems seem to be inconsistent. Li and Weaver [15] and Forster and Faulkner [17] obtained $\beta_{exp} \approx 1.6$ Å^{-1} for redox centers covalently linked to the end groups of monolayers adsorbed to gold or platinum electrodes. However, Finklea and Hanshew [95] and Carter et al. [18] obtained $\beta_{exp} \approx 0.97$ Å^{-1} for other redox groups also attached to monolayers adsorbed to the surface of gold electrodes. The discrepancy between the β_{exp} values of these systems is at variance with the similarity between their tunneling barrier heights and the molecular structures of the monolayers. Apparently, the only difference between the two sets of values is the length of the bridges: in the first set they are smaller than 10 Å. This type of difference is usually associated with a change in mechanism, from through-space tunneling for the shorter bridges to through-bond tunneling in the longer bridges. Actually, our tunneling model is consistent with the larger tunneling decay coefficients, which gives support to a through-space mechanism in the shorter bridges. However, there is no fundamental reason why a through-space mechanism operating in metal–adsorbed monolayer–metal junctions with monolayers up to 30 Å in length would be inefficient in unimolecular electrochemical transfers through smaller bridges. A clue to this puzzle can be found in the recent temperature dependence studies performed by Carter et al. [18]. The real distance dependence of the electronic coupling must be obtained from a plot of the pre-exponential term as a function of the bridge length in

Table 5
Parameters of ISM employed in the calculations of the intramolecular ET rates shown in Figs. 3–7 [a]

Reactant [b]	$n^{\ddagger}$	$l_r + l_p$ (pm)	f_r (J mol^{-1} pm^{-2})	f_p (J mol^{-1} pm^{-2})	T (K)	χ_0	β_{calc} [c] (pm^{-1})	λ (kJ mol^{-1})	ΔG^0 (kJ mol^{-1})
Bi$^-$–{cycloalkyl}-Na	1.435	280	377	377	296	1	0.0106	140	−4.8
DMNa*–{norbornyl}–DCE	1.65	270	499	483	298	1	0.0104	140	−122.5
ZnTTP*–{spirocyclic}–AQ	1.67	341	278	278	298	1	0.0134	100	−52
(bpy)$_2$Ru-bpy*–{alkyl}–MV	1.45	276	389	389	296	6.4×10^{-2}	0.0143	100	−49
MV–{alkyl}–Ru(bpy)$_3$	1.69	342	362	362	296	1	0.0066	120	
(NH$_3$)$_5$Os-py$^-$–{pro}–OCo(NH$_3$)$_5$	1.19	344	393	309	298	10^{-3}	0.0153	350	−15
(NH$_3$)$_5$Os-py$^-$–{pro}–ORu(NH$_3$)$_5$	1.42	350	403	360	298	1	0.0153	350	−24
(bpy)$_2$Ru-bpy*–{pro}–OCo(NH$_3$)$_5$	1.18	345	370	286	293	10^{-3}	0.0144	350	−68
(bpy)$_2$Ru-bpy$^-$–{pro}–OCo(NH$_3$)$_5$	1.18	345	370	286	293	10^{-3}	0.0128	350	−106

[a] The transition state bond order was calculated with Eq. (6) using the bond orders of the reactants and products given in Table 4; the bond lengths and force constants are the average values of the data for the reactants and products given in Table 4.
[b] Bi, biphenyl; Na, naphthalene; DMNa, dimethoxynaphthalene; DCE, dicyanovinyl; AQ, anthraquinone; MV, methylviologen; the other abbreviations are given in Table 1 and Table 3.
[c] From data in Table 1 and Table 3.

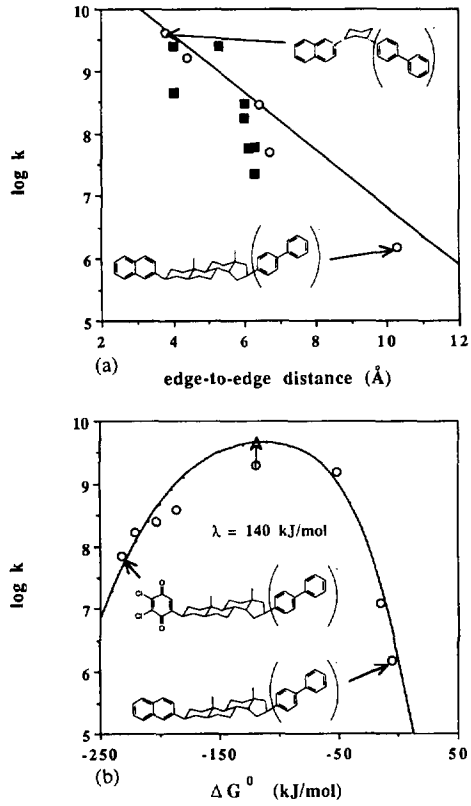

Fig. 7. Experimental and calculated intramolecular ET rates from biphenylyl anion to aromatic acceptors across rigid bridges made of saturated cyclic hydrocarbon chains. Data from Table 5. (a) Distance dependence in tetrahydrofuran showing donor and acceptor in equatorial positions (○) or other conformations (■); no parameters were adjusted in these calculations. (b) Free energy dependence in methyltetrahydrofuran reproduced with the adjustment of only one parameter, λ.

order to factor out the distance dependence of the nuclear factor. When this is performed, the experimental tunneling decay coefficient is in good agreement with that calculated with our tunneling model (Table 2). The data on Al–monolayer–Al junctions at 293 and 77 K indicate that, for this type of system, β_{exp} has only a small temperature dependence.

A similar distinction between the distance dependence of the nuclear and electronic factors can be made in systems in which prolines are used as spacers. In donor–oligoproline–acceptor systems, the distance dependence of the ET rates has been investigated for edge-to-edge distances ranging from 1.4 to 29.3 Å [100]. These distances were estimated by taking 1.4 Å as the distance in the absence of prolines, and adding 3.1 Å for each proline unit introduced in the bridge [100]. A non-linear dependence of $\ln k$ vs. distance was observed in these systems. There is some arbitrariness in choosing the initial and final slopes of non-linear plots but, for the system (bpy)$_2$Ru^{II}-bpy$^-$–[proline]$_{1-6}$–ROCo^{III}-(NH$_3$)$_5$, they seem to be 1.3 Å^{-1} and 0.3 Å^{-1} respectively. Our tunneling model predicts a non-linear distance dependence of the logarithm of the intramolecular ET rates, because the refractive index increases with the size of the molecules. The calculated tunneling decay coefficients are in good agreement with the experimental values when the bridges are made

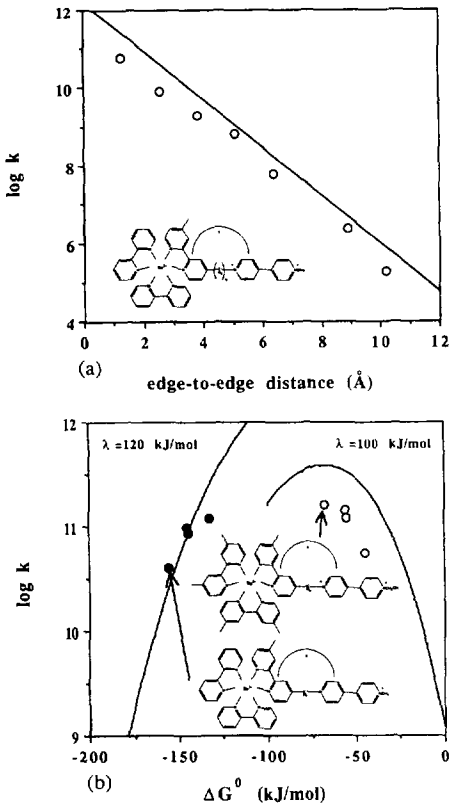

Fig. 8. Experimental (○) and calculated photoinduced intramolecular ET rates in acetonitrile of a series of ruthenium trisbipyridyl–methylviologen donor–acceptor molecules covalently linked by flexible aliphatic spacers. Data from Table 5. (a) Distance dependence calculated without adjustable parameters. (b) Free energy dependence also showing the thermal "hole" transfer in the same system (●); the ET rates are not appreciably sensitive to λ, the only empirical parameter employed in the calculations; the "hole" transfer rates were calculated with the empirical distance dependence of the rates and with the adjustment of λ.

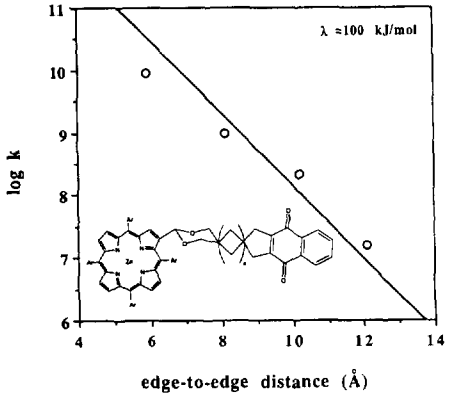

Fig. 9. Experimental and calculated distance dependence of photoinduced intramolecular ET rates in *n*-butanol of zinc tetratolylporphyrin–quinone donor–acceptor molecules covalently linked by rigid homologous spirocyclic spacers. Data in Table 5. The calculations are not very sensitive to the empirical parameter λ, and its value was taken from Fig. 8(b).

of three or less proline units (Table 3). However, the decrease in β_{exp} with increasing chain length exceeds that expected from the tunneling model, and for longer bridges, which have a helical structure, the model overestimates the distance dependence of the ET rates. This deviation is not

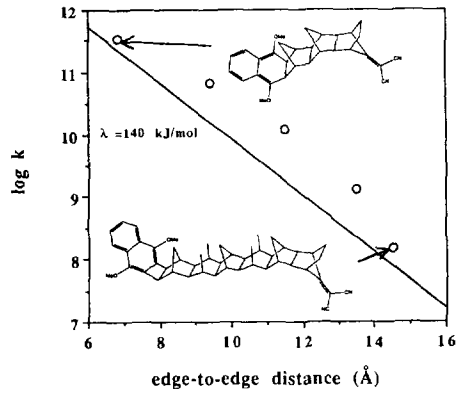

Fig. 10. Experimental and calculated distance dependence of photoinduced intramolecular ET rates in tetrahydrofuran of dimethoxynaphthalene–dicyanoethylene donor–acceptor molecules covalently linked by rigid polynorbornyl spacers. Data in Table 5. The calculations are sensitive to the empirical parameter λ, but its value can be transferred from Fig. 7(b).

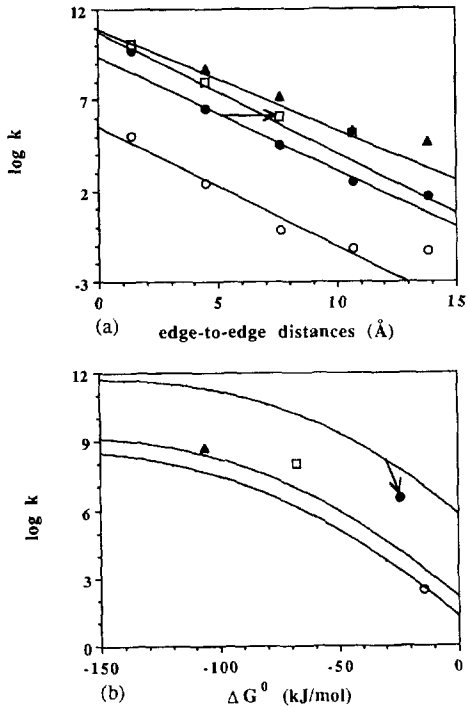

Fig. 11. Experimental and calculated intramolecular ET rates in water of osmium or ruthenium complexes to cobalt or ruthenium complexes covalently linked by oligoproline spacers. The Os → Ru, Os → Co and Ru → Co thermal ETs are represented by ○, ● and ▲ respectively; the photochemical Ru → Co ETs are represented by □. Data in Table 5. (a) Distance dependence of the ET rates; only the calculations on Ru → Co ET are appreciably dependent on the adjustable parameter λ. (b) Free energy dependence of the ET rates with one proline as spacer; the value of λ was adjusted.

entirely due to the distance dependence of the nuclear factor when the bridges are longer than 10 Å, because the tunneling barriers involved only yield $\beta_{el} \approx 0.5$ Å^{-1} if $n_D = 3.69$. We are not aware of the existence of systems with such high refractive indices. The determination of β_{el} from $-\Delta S^{\ddagger}/R$ vs. distance plots rests on several assumptions [101], whose validity is more difficult to assess for these systems than for electrochemical ET. This advises against a detailed analysis of these decay coefficients. Rather than speculating on their

values, we wish to emphasize the following points: (1) there is reasonable agreement between β_{exp} and β_{calc} before the onset of the helical structure; (2) the decrease in β_{el} with chain length is much less pronounced than the decrease in β_{exp}, and approaches that expected for β_{calc}; (3) ET through helical oligopeptides has a smaller distance dependence than expected from our tunneling model, suggesting a lower energy conduction band for ET in these systems.

In summary, of the four types of ET system addressed in this work (donor–bridge–acceptor, donor–rigid matrix–acceptor, metal–monolayer–metal, electrode–monolayer–redox center), only the bridges made of helical oligoprolines seem to have a smaller distance dependence than that calculated by our tunneling model. Next, we discuss the association of this tunneling model with ISM to calculate ET rates in intramolecular donor–bridge–acceptor systems.

The intramolecular ET from the biphenylyl anion to a naphthyl group in rigid molecules, originally studied by Closs et al. [13], is ideally suited to test the semiclassical formulation of ISM with neglect of reaction free energy effects, because for these reactions $\Delta G^0 \approx -5$ kJ mol^{-1}. Under this approximation, absolute rate constant calculations were performed and the results are shown in Fig. 7(a). There is some scatter in the experimental data shown, because this refers to different conformations of the electron donor or acceptor. The scatter illustrates the fact that conformational effects may account for an order of magnitude variation in the rates. There is a very good agreement between the rates calculated without adjustable parameters and the experimental rates measured for donors and acceptors in equatorial positions of the bridge. The effects of the conformations of the donors and acceptors on the ET rates are not explicitly accounted for in the present formulation of semiclassical ISM. Nevertheless, the absolute calculations of the rates are within an order of magnitude of the experimental values.

The free energy effects on the reaction rates and, in particular, the Marcus inverted region, clearly observed for the first time in these systems, can be modelled by introducing one adjustable parameter, λ. Its value of $\lambda = 140$ kJ mol^{-1} was obtained by fitting Eq. (5), Eq. (9a), Eq. (9b) and Eq. (18) to the experimental ET rates in MTHF when the biphenyl anion is the donor, the bridge is a steroid and a variety of acceptors are used. The non-adiabatic factor χ_R employed in these calculations was obtained from Eq. (10). Our fit to the experimental rates is shown in Fig. 7(b). The interpretation of Closs et al. [13] of this free energy profile based on the golden rule expression, to be discussed below, required the use of four adjustable parameters.

Absolute calculations were also performed for photoinduced ET in the covalently linked ruthenium tris(bipyridyl)–viologen molecules studied by Yonemoto et al. [82]. ET occurs only from a metal-to-ligand charge transfer (MLCT) state localized on the bipyridine ligand linked to the acceptor. The fraction of MLCT states is 0.064 [119], and so this value was selected for χ_0. Fig. 8(a) shows the calculated and experimental rates at different donor–acceptor separations. They are within a factor of five from each other with $\lambda = 100$ kJ mol^{-1} and are not very sensitive to this parameter. The reaction free energy dependence of the ET rates in systems making use of similar donors and acceptors separated by a CH_2 linkage is shown in Fig. 8(b). The rates shown in this figure correspond to two distinct situations: in the "normal" rate region, an electron is transferred from an MLCT state to a viologen acceptor; in the "inverted" rate region, the negative charge returns from the viologen to the ruthenium complex. The latter can also be interpreted as the transfer of a hole from the ruthenium complex to the viologen. These "electron" or "hole" transfers differ in terms of the parameters characterizing the reactants, the distances between donor and acceptor and the tunneling decay coefficients. The photochemical ET occurs at moderate ΔG^0 values and the calculation of the rate is not very sensitive to the value of λ. Thus the comparison between the experimental and calculated photochemical ET rates in Fig. 8(b) must be guided by the fact that no parameters were adjusted in our calculations. Again, the calculated and experimental rates agree within a factor of five. The fits presented by Yonemoto et al. [82] using the golden rule expression involved the adjustment of three parameters in the normal region and four parameters in the inverted region. The application of semiclassical ISM to this system is an important advance in terms of predictability and physical insight.

The reactants in the "hole" transfer in these systems are the $Ru(bpy)_3^{3+/2+}$ complex and methylviologen. The parameters representing these reactants are given in Table 4 and Table 5. Absolute calculations of the "hole" transfer rates are not possible because these reactions occur at very negative ΔG^0 values and their rates are very sensitive to the value of λ. Thus it is not justifiable to make an effort to calculate hole frequencies and decay coefficients for this system. Instead, in our calculations, we employed the empirical distance dependence of the hole transfers [82], estimated R_e by adding 3.45 Å to the R_e value of photochemical ET in these systems to account for the size of the ligand in the complex and used the same frequency for electron and "hole" transfers. In Fig. 8(b), we compare the free energy dependence of the experimental and calculated rates when λ is set to 120 kJ mol^{-1}. A larger value of λ would lead to faster rates and a flatter log k vs. ΔG^0 profile. A smaller λ would lead to slower rates and a steeper log k vs. ΔG^0 profile. The selected value of λ gives a good agreement both with the absolute magnitude of the rates and their ΔG^0 dependence, indicating that the reaction coordinate was well chosen.

The absolute rate constant calculations presented in Fig. 9 are a straightforward application of ISM to the photoinduced porphyrin-to-quinone ET across oligospirocyclic spacers [83]. No parameters had to be adjusted to obtain agreement between the calculated and experimental rates. We set $\lambda = 100$ kJ mol^{-1} for consistency with Fig. 8(b). The bond order of the zinc tetratolylporphyrin complex was taken as $n^{\ddagger} = 2$, by analogy with the metal–bipyridine bond order in bipyridine and phenanthroline complexes of transition metals [31,36].

The photoinduced dimethoxynaphthalene-to-dicyanovinyl ET across polynorbornyl bridges, studied by Oevering et al. [81], has moderately low ΔG^0 values. The effect of λ on the reaction rates cannot be neglected and its value must be estimated. These systems and those studied by Closs et al. [13] are structurally similar. Therefore it can be expected that the value of λ employed to reproduce the rate constants measured in MTHF by Closs et al. [13] should be transferable to the rates measured in THF by Oevering et al. [81]. The calculations shown in Fig. 10 were made with $\lambda = 140$ kJ mol^{-1} and they agree with the experimental rates within a factor of five. These results show that the empirical value of λ can be estimated from similar systems, confirming the consistency and predictability of the model.

The ET rate in the system $(NH_3)_5Os$-py-$\{pro\}_{0-4}$-$ORu(NH_3)_5$ can also be calculated without adjustable parameters. In the calculations shown in Fig. 11, we considered that the electron being transferred is localized in the pyridine ligand of the osmium complex. Thus the parameters representing the reactants and products are the average of those of pyridine and $(H_2O)Ru(NH_3)_5$. For bridges involving three or less proline units, the calculated rates are within an order of magnitude of the experimental values [99] in a system in which the rate constants span over a range of eight orders of magnitude.

Some ET reactions presented in Fig. 11 involve spin-forbidden exchanges at cobalt centers. As mentioned in Section 1, recent experimental and theoretical evidence indicates that high-spin to low-spin exchanges in cobalt complexes must have spin-forbidden factors of approximately 10^{-3}. We included such factors in the calculations presented in this figure. As such factors were not calculated by our model, we do not claim that our calculations on these systems are "absolute". They are, however, entirely consistent with our earlier work on intermolecular electron self-exchanges and cross-relations involving cobalt complexes.

We can analyse the free energy dependence of intramolecular ET across prolines in aqueous solutions using the rates measured by Isied and coworkers [100] when the donor and acceptor are separated by one proline unit. The reactants cannot be characterized by a single set of parameters, because they are structurally different. Thus in Fig. 11(b), we present three different calculated curves, corresponding to the parameters of: (i) pyridine$^{-/0}$ and $(H_2O)Co^{III/II}(NH_3)_5$; (ii) pyridine$^{-/0}$ and $(H_2O)Ru^{III/II}(NH_3)_5$; (iii) bipyridine$^{-/0}$ and $(H_2O)Co^{III/II}(NH_3)_5$. The calculations on the two most exothermic systems presented in this figure are appreciably dependent on the value of λ. The adjusted value of λ is 350 kJ mol^{-1}. The improved agreement with the experimental rates when different parameters are used to represent the reactants shows that ΔG^0 is not the only relevant parameter which varies in this series of reactions, i.e. the series is not homogeneous. The value of λ found in these systems is significantly higher than that for the other intramolecular ET reactions studied here, but is similar to that found in intermolecular ET in aqueous solution [36]. A similar increase from 148 kJ mol^{-1} in cyclohexane to 200 kJ mol^{-1} in acetonitrile has been reported for ET quenching of excited state fluorophores [53]. The increase in the value of λ is associated with a better coupling between reactive and non-reactive modes, which facilitates the accommodation of the reaction exothermicity in the non-reactive modes. This picture is compatible with the larger values of λ for reactions of ionic species in more polar solvents.

Our calculations may be compared with those making use of Fermi's golden rule derived from quantum mechanical perturbation theory. According to this rule, the ET rate is written as a product of an electronic and a nuclear factor

$$k_{gr} = \frac{2\pi}{\hbar} V_R^2 FC \tag{24}$$

where V_R^2 is the distance-dependent coupling between reactant and product electronic wavefunctions and FC represents the Franck–Condon factor derived from the overlap of the nuclear wavefunctions. The Franck–Condon factor explicitly depends on three parameters: the solvent reorganization energy (λ_S), the internal reorganization energy (λ_i) and an averaged frequency of typical skeletal vibrations (ω). The dielectric continuum model developed by Marcus can be used to estimate the value of λ_S. The value of 1500 cm^{-1} is sometimes adopted for ω. For each series of ET reactions, the values of λ_i and the electronic coupling matrix element (V_R) are obtained from the fitting of Eq. (24) to the experimental profile of the ET rates vs. reaction free energies. A good fit of the free energy dependence of the ET rates usually requires the adjustment of the four parameters mentioned above [80,82,120–122]. The use of Eq. (24) to fit simultaneously the free energy and distance dependence of intramolecular ET rates in rigid systems requires the knowledge of a fifth parameter (the tunneling decay coefficient β) and, to our knowledge, has not been attempted. Thus the application of Eq. (24) to the free energy and distance dependence of these systems normally requires empirical estimates of $V_{R=0}$, β, λ_S, λ_i and ω. The application of ISM requires only one empirical parameter, λ, which we keep constant for similar reactions in the same reaction conditions. Although it is not fair to compare the quality of the fit obtained by a model with five adjustable parameters with that of another model using only one adjustable parameter, the quality of the fit obtained with ISM is at least comparable with the quality of the fit obtained by Eq. (24).

The results of our absolute rate calculations on these intramolecular ET reactions are very encouraging and suggest that it should also be possible to perform similar absolute rate calculations on intermolecular σ^*-d electron transfers in transition metal complexes. Earlier attempts to make such calculations were hindered by the non-adiabaticity of these reactions, and required the empirical estimate of the corresponding non-adiabatic factors [31,36]. These factors were estimated to range from $\chi_R = 10^{-2}$, for exchanges involving hexaaquo complexes, to $\chi_R = 10^{-6}$, for tris(2,2′-bipyridyl)

complexes. We can now estimate the distance-dependent non-adiabatic factors of σ^*-d ET using our tunneling model. The edge-to-edge distance in these complexes is given by

$$R_e = R_c - l_{ox} - l_{red} \quad (25)$$

where R_c is the metal–metal distance in the activated complex and l_{ox} and l_{red} are the metal–ligand bond lengths. The tunneling barriers are determined by the absolute thermodynamic potentials of the oxidation–reduction couples (E^0) [123], divided by the square of the refractive index of the ligands. Using $E^0 = -0.41$ V vs. NHE for $Cr(H_2O)^{3+/2+}$ and $E^0 = 1.51$ V vs. NHE for $Mn(H_2O)^{3+/2+}$, with the absolute thermodynamic potential of NHE ($\Phi^0 = 4.44$ eV) and $n_D = 1.333$ for water, we obtain $2.7 \times 10^{-2} \leq \chi_R \leq 1.2 \times 10^{-2}$. Similarly, using $E^0 = 1.72$ V vs. NHE for $Ni(bpy)^{3+/2+}$ and $E^0 = 0.36$ V vs. NHE for $Co(phen)^{3+/2+}$, we obtain, with $n_D = 1.62$ for bipyridyl, $3.1 \times 10^{-7} \leq \chi_R \leq 1.7 \times 10^{-6}$. The agreement between the calculated and empirical χ_R values shows that it is possible to use ISM to make absolute calculations of intermolecular σ^*-d electron transfers in transition metal complexes.

The only caveat concerning applications of ISM to ET is the difference between intramolecular and intermolecular frequencies: the former is an electronic frequency approximately two orders of magnitude larger than the latter, which is a nuclear frequency.

5. Conclusions

This work has shown that the distance dependence of ET in a wide variety of rigid systems can be treated as electron tunneling from the donor to the acceptor through a square potential barrier. The length of the tunneling barrier is given by the donor–acceptor edge-to-edge distance. The height of the barrier can be calculated as the difference between the energy of the electron at rest in a vacuum and its energy in the donor, divided by the optical dielectric constant of the medium crossed by the electron. This accounts for the dielectric stabilization of the electron energy by the molecular properties of the medium. This tunneling model and the electronic frequency factor, $\nu_{el} = 5 \times 10^{14}$ s^{-1}, can be associated with ISM to calculate the rate of intramolecular ET in rigid systems, if the electron initially occupies a delocalized π^* molecular orbital of the donor. For reactions with $|\Delta G^0| < 50$ kJ mol^{-1}, it is possible to make absolute calculations of intramolecular ET rates which are within one order of magnitude of the experimental rates. The tunneling model also provides a rationale for the empirical non-adiabatic factors found in earlier applications of ISM to σ^*-d electron exchanges between transition metal complexes.

The picture that emerges from our applications of ISM to ET reactions of transition metal complexes and organic species is that absolute rate calculations can be made if the force constants, bond lengths and bond orders of the reactants are known and if the reaction free energies are not very negative. For very exothermic ET, the calculations involve an empirical parameter λ, which is constant for reactions involving similar reactants and solvents and is related to the dynamics of the reaction.

Acknowledgements

We are grateful to Junta Nacional de Investigação Científica e Tecnológica and Praxis XXI (European Union) for financial support (Project No. Praxis/2/2.1/QU1/390/94).

References

[1] J. Deisenhofer, O. Epp, K. Miki, R. Hubber and H. Michel, *J. Mol. Biol., 180* (1984) 385.
[2] J.S. Connolly and J.R. Bolton, in M.A. Fox and M. Chanon (eds.), *Photoinduced Electron Transfer*, Elsevier, Amsterdam, 1988, p. 303.
[3] J.R. Reimers, J.S. Craw and N.S. Hush, in A. Aviram (ed.), *Molecular Electronics—Science and Technology*, US Engineering Foundation, New York, 1992, p. 11.
[4] B. Mann and H. Kuhn, *J. Appl. Phys., 42* (1971) 4398.
[5] H. Kuhn, *J. Photochem., 10* (1979) 111.
[6] H. Kuhn, *Pure Appl. Chem., 51* (1979) 341.
[7] D. Möbius, *Acc. Chem. Res., 14* (1981) 63.
[8] H. Kuhn, *Thin Solid Films, 178* (1989) 1.
[9] J.R. Miller, *J. Chem. Phys., 56* (1972) 5173.
[10] J.R. Miller, *Science, 189* (1975) 221.
[11] J.R. Miller, J.V. Beitz and R.K. Huddleston, *J. Am. Chem. Soc., 106* (1984) 5057.
[12] V.V. Krongauz, *J. Phys. Chem., 96* (1992) 2609.
[13] G.L. Closs, L.T. Calcaterra, N.J. Green, K.W. Penfield and J.R. Miller, *J. Phys. Chem., 90* (1986) 3673.
[14] C.K. Ryu, R. Wang, R.H. Schmehl, S. Ferrere, M. Ludwikow, J.W. Merkert, C.E. Headford and C.M. Elliott, *J. Am. Chem. Soc., 114* (1992) 430.
[15] T.T.-T. Li and M.J. Weaver, *J. Am. Chem. Soc., 106* (1984) 6107.
[16] L.H. Dubois and R.G. Nuzzo, *Annu. Rev. Phys. Chem., 43* (1992) 437.
[17] R.J. Forster and L.R. Faulkner, *J. Am. Chem. Soc., 116* (1994) 5444.
[18] M.T. Carter, G.K. Rowe, J.N. Richardson, L.M. Tender, R.H. Terrill and R.W. Murray, *J. Am. Chem. Soc., 117* (1995) 2896.
[19] C.C. Moser, J.M. Keske, K. Warncke, R.S. Farid and P.L. Dutton, *Nature, 355* (1992) 796.
[20] S. Woitellier, J.P. Launay and C.W. Spangler, *Inorg. Chem., 28* (1989) 758.
[21] M.D. Ward, *Chem. Soc. Rev.*, (1995) 121.
[22] H.M. McConnell, *J. Chem. Phys., 35* (1961) 508.
[23] R. Hoffmann, *Acc. Chem. Res., 4* (1971) 1.
[24] M.N. Paddon-Row, *Acc. Chem. Res., 27* (1994) 18.
[25] K. Kim, K.D. Jordan and M.N. Paddon-Row, *J. Phys. Chem., 98* (1994) 11 053.
[26] L.A. Curtiss, C.A. Naleway and J.R. Miller, *J. Phys. Chem., 99* (1995) 1182.
[27] S. Larsson and M. Braga, *J. Photochem. Photobiol. A: Chem., 82* (1994) 61.
[28] C. Liang and M.D. Newton, *J. Phys. Chem., 97* (1993) 3199.
[29] P.W. Anderson, *Phys. Rev., 79* (1950) 350.
[30] M.D. Newton and N. Sutin, *Annu. Rev. Phys. Chem., 35* (1984) 437.

[31] S.J. Formosinho and L.G. Arnaut, *J. Mol. Struct. (Theochem.), 130* (1994) 105.
[32] X. Song, Y. Lei, S. Van Wallendal, M.W. Perkovic, D.C. Jackman, J.F. Endicott and D.P. Rillema, *J. Phys. Chem., 97* (1993) 3225.
[33] E. Buhks, M. Bixon, J. Jortner and G. Navon, *Inorg. Chem., 18* (1979) 2014.
[34] S. Larsson, K. Ståhl and M.C. Zerner, *Inorg. Chem., 25* (1986) 3033.
[35] M.D. Newton, *J. Phys. Chem., 95* (1991) 30.
[36] S.J. Formosinho and L.G. Arnaut, *J. Photochem. Photobiol. A: Chem., 82* (1994) 11.
[37] S.J. Formosinho and L.G. Arnaut, *Bull. Chem. Soc. Jpn.*, in press.
[38] A.J.C. Varandas and S.J. Formosinho, *J. Chem. Soc., Faraday Trans. 2, 82* (1986) 953.
[39] A.J.C. Varandas and S.J. Formosinho, *J. Chem. Soc., Chem. Commun.*, (1986) 163.
[40] S.J. Formosinho, in S.J. Formosinho, I.G. Csizmadia and L.G. Arnaut (eds.), *Theoretical and Computational Models for Organic Chemistry*, NATO ASI, Kluwer, Dordrecht, 1991, p. 159.
[41] S.J. Formosinho, *J. Chem. Soc., Perkin Trans. 2,* (1987) 61.
[42] S.J. Formosinho and V.M.S. Gil, *J. Chem. Soc., Perkin Trans. 2,* (1987) 1655.
[43] L.G. Arnaut and S.J. Formosinho, *J. Phys. Chem., 92* (1988) 685.
[44] S.J. Formosinho and L.G. Arnaut, *J. Chem. Soc., Perkin Trans. 2,* (1989) 1947.
[45] K. Yates, *J. Phys. Org. Chem., 2* (1989) 300.
[46] L.G. Arnaut and S.J. Formosinho, *J. Phys. Org. Chem., 3* (1990) 95.
[47] L.G. Arnaut, *J. Phys. Org. Chem., 4* (1991) 726.
[48] L.G. Arnaut, in T. Bountis (ed.), *Proton Transfer in Hydrogen-Bonded Systems*, Plenum, New York, 1992, p. 281.
[49] L.G. Arnaut and S.J. Formosinho, *J. Photochem. Photobiol. A: Chem., 69* (1992) 41.
[50] L.G. Arnaut and S.J. Formosinho, *J. Photochem. Photobiol. A: Chem., 75* (1993) 1.
[51] S.J. Formosinho, *J. Chem. Soc., Perkin Trans. 2,* (1988) 1209.
[52] S.J. Formosinho, *Pure Appl. Chem., 61* (1989) 891.
[53] L.G. Arnaut and S.J. Formosinho, *J. Mol. Struct. (Theochem.), 233* (1991) 209.
[54] L.G. Arnaut, in A.J.L. Pombeiro and J. McCleverty (eds.), *Molecular Electrochemistry of Inorganic, Bioinorganic and Organometallic Compounds*, NATO ASI Series, Kluwer, Dordrecht, 1993, p. 207.
[55] S.F. Nelsen, D.T. Rumack and M. Meot-Ner (Mautner), *J. Am. Chem. Soc., 109* (1987) 1373.
[56] D.K. Phelps, J.R. Gord, B.S. Freiser and M.J. Weaver, *J. Phys. Chem., 95* (1991) 4338.
[57] G.E. McManis, R.M. Nielson, A. Gochev and M.J. Weaver, *J. Am. Chem. Soc., 111* (1989) 5533.
[58] M.-S. Chan and A.C. Wahl, *J. Phys. Chem., 86* (1982) 126.
[59] T.T.-T. Li and C.H. Brubaker, Jr., *J. Organomet. Chem., 216* (1981) 223.
[60] R.M. Nielson, J.T. Hupp and D.I. Yoon, *J. Am. Chem. Soc., 117* (1995) 9085.
[61] G. Rauhut and T. Clark, *J. Am. Chem. Soc., 115* (1993) 9127.
[62] G. Rauhut and T. Clark, *J. Chem. Soc., Faraday Trans., 90* (1994) 1783.
[63] B.S. Brunschwig, C. Creutz, D.H. Macartney, T.-K. Sham and N. Sutin, *Faraday Discuss. Chem. Soc., 74* (1982) 113.
[64] N. Sutin, *Prog. Inorg. Chem., 30* (1983) 441.
[65] D.G. Truhlar and B.C. Garrett, *Annu. Rev. Phys. Chem., 35* (1984) 159.
[66] G.F. Johnson and A.C. Albrecht, *J. Chem. Phys., 44* (1966) 3179.
[67] B. Katz, M. Brith, B. Sharf and J. Jortner, *J. Chem. Phys., 50* (1969) 5195.
[68] S. Lipsky, *J. Chem. Ed., 58* (1981) 93.
[69] B.E. Spingett, J. Jortner and M.H. Cohen, *J. Chem. Phys., 48* (1968) 2720.
[70] R.A. Holroyd, *J. Chem. Phys., 57* (1972) 3007.
[71] R.P. Bell, *The Tunnel Effect in Chemistry*, Chapman and Hall, London, 1980, pp. 39, 43.
[72] G. Binnig, H. Rohrer, C. Gerber and E. Weibel, *Physica, 109/110B* (1982) 2075.
[73] G. Binnig and H. Rohrer, *Angew. Chem. Int. Ed. Engl., 26* (1987) 606.
[74] J.V. Beitz and J.R. Miller, *J. Chem. Phys., 71* (1979) 4579.
[75] R.O. Loutfy and R.O. Loutfy, *Can. J. Chem., 54* (1976) 1454.
[76] S. Trasatti, *Pure Appl. Chem., 58* (1986) 955.
[77] T. Heinis, S. Chowdhury, S.L. Scott and P. Kebarle, *J. Am. Chem. Soc., 110* (1988) 400.
[78] A.M. Becka and C.J. Miller, *J. Phys. Chem., 96* (1992) 2657.
[79] J.G. Simons, *J. Appl. Phys., 34* (1963) 1793.
[80] B. Paulson, K. Pramod, P. Eaton, G. Closs and J.R. Miller, *J. Phys. Chem., 97* (1993) 13 042.
[81] H. Oevering, M.N. Paddon-Row, M. Heppener, A.M. Oliver, E. Cotsaris, J.W. Verhoeven and N.S. Hush, *J. Am. Chem. Soc., 109* (1987) 3258.
[82] E.H. Yonemoto, G.B. Saupe, R.H. Schmehl, S.M. Hubig, R.L. Riley, B.L. Iverson and T.E. Mallouk, *J. Am. Chem. Soc., 116* (1994) 4786.
[83] S. Knapp, T.G. Murali Dhar, J. Albaneze, S. Gentemann, J.A. Potenza, D. Holten and H.J. Schugar, *J. Am. Chem. Soc., 113* (1991) 4010.
[84] B.A. Leland, A.D. Joran, P.M. Felker, J.J. Hopfield, A.H. Zewail and P.B. Dervan, *J. Phys. Chem., 89* (1985) 5571.
[85] A. Helms, D. Heiler and G. McLendon, *J. Am. Chem. Soc., 114* (1992) 6227.
[86] S. Strauch, G. McLendon, M. McGuire and T. Guarr, *J. Am. Chem. Soc., 87* (1983) 3579.
[87] I.V. Alexandrov, R.F. Khairutdinov and K.I. Zamataev, *Chem. Phys., 32* (1978) 123.
[88] K.I. Zamaraev, R.F. Khairutdinov and J.R. Miller, *Chem. Phys. Lett., 57* (1978) 311.
[89] Y. Sakata, H. Tsue, M.P. O'Neil, G.P. Wiederrecht and M.R. Wasielewski, *J. Am. Chem. Soc., 116* (1994) 6904.
[90] T. Guarr, M. McGuire, S. Strauch and G. McLendon, *J. Am. Chem. Soc., 105* (1983) 616.
[91] J.R. Miller, *Chem. Phys. Lett., 22* (1973) 180.
[92] E.E. Polymeropoulos and J. Sagiv, *J. Chem. Phys., 69* (1978) 1836.
[93] E.E. Polymeropoulos, *J. Appl. Phys., 48* (1977) 2404.
[94] M. Sugi, Y. Fukui and S. Iizima, *Appl. Phys. Lett., 27* (1975) 559.
[95] H.O. Finklea and D.D. Hanshew, *J. Am. Chem. Soc., 114* (1992) 3173.
[96] S. Trasatti, *Adv. Electrochem. Electrochem. Eng., 10* (1977) 213.
[97] W. Groh and A. Zimmermann, *Macromolecules, 24* (1991) 6660.
[98] S.S. Isied, A. Vassilian, R.H. Magnuson and H.A. Schwarz, *J. Am. Chem. Soc., 107* (1985) 732.
[99] A. Vassilian, J.F. Wishart, B. van Hemelryck, H. Schwarz and S.S. Isied, *J. Am. Chem. Soc., 112* (1990) 7278.
[100] S.S. Isied, M.Y. Ogawa and J.F. Wishart, *Chem. Rev., 92* (1992) 381.
[101] M.Y. Ogawa, J.F. Wishart, Z. Young, J.R. Miller and S.S. Isied, *J. Phys. Chem., 97* (1993) 1156.
[102] M.Y. Ogawa, I. Moreira, J.F. Wishart and S.S. Isied, *Chem. Phys., 176* (1993) 589.
[103] N. Neto, M. Scrocco and S. Califano, *Spectrochim. Acta, 22* (1966) 1981.
[104] J.L. Baudor and M. Sanquer, *Acta Crystallogr., Teil B, 39* (1983) 75.
[105] G. Zerbi and S. Sandroni, *Spectrochim. Acta, Part A, 24* (1968) 511.
[106] J. Trotter, *Acta Crystallogr., 13* (1960) 86.
[107] K.S. Raymond and R.A. Wheeler, *J. Chem. Soc., Faraday Trans., 89* (1993) 665.
[108] L.O. Peitilä, K. Palmö and B. Mannfors, *J. Mol. Spectrosc., 116* (1986) 1.
[109] D.M. Chipman and M.F. Prebenda, *J. Phys. Chem., 90* (1986) 5557.
[110] L.L. Merritt, Jr. and E.D. Schroeder, *Acta Crystallogr., 9* (1956) 801.

[111] N. Neto, M. Muniz-Miranda, L. Angeloni and E. Castellucci, *Spectrochim. Acta, Part A, 39* (1982) 97.
[112] S. Ghoshal, T. Lu, Q. Feng and T.M. Cotton, *Spectrochim. Acta, Part A, 44* (1988) 651.
[113] D.A. Dixon and J.S. Miller, *J. Am. Chem. Soc., 109* (1987) 3656.
[114] J.J. Hinkel and J.P. Devlin, *J. Chem. Phys., 58* (1973) 4750.
[115] B. Bak, L. Hansen-Nygaard and J. Rastrup-Andersen, *J. Mol. Spectrosc., 2* (1958) 31.
[116] J.W. Emsley, J.C. Lindon and J. Tabony, *J. Chem. Soc., Faraday Trans. 2, 71* (1975) 579.
[117] W.R. Scheidt, M.E. Kastner and K. Hatano, *Inorg. Chem., 17* (1978) 706.
[118] Y. Saito, J. Takemoto, B. Hutchinson and K. Nakamoto, *Inorg. Chem., 11* (1972) 2003.
[119] L.F. Cooley, C.E.L. Headford, C.M. Elliott and D.F. Kelley, *J. Am. Chem. Soc., 110* (1988) 6673.
[120] T. Asahi, M. Ohkohchi, R. Matsusaka, N. Mataga, R.P. Zhang, A. Osuka and K. Maruyama, *J. Am. Chem. Soc., 115* (1993) 55.
[121] H. Heitele, F. Pöllinger, T. Härberle, M.E. Michel-Beyerle and H.A. Staab, *J. Phys. Chem., 98* (1994) 7402.
[122] L.R. Khundkar, J.W. Perry, J.E. Hanson and P.B. Dervan, *J. Am. Chem. Soc., 116* (1994) 9700.
[123] D.E. Richardson, *Inorg. Chem., 29* (1990) 3213.